INTERNATIONAL JOURNAL OF CLIMATOLOGY
Int. J. Climatol. (2017)
Published online in Wiley Online Library
(wileyonlinelibrary.com) DOI: 10.1002/joc.5252

RMetS
Royal Meteorological Society

Projected changes in mean rainfall and temperature over East Africa based on CMIP5 models

Victor Ongoma,[a,b,c]* Haishan Chen[a,b] and Chujie Gao[a,b]

[a] *Collaborative Innovation Center on Forecast and Evaluation of Meteorological Disasters (CIC-FEMD)/Key Laboratory of Meteorological Disaster, Ministry of Education (KLME), Nanjing University of Information Science & Technology (NUIST), China*
[b] *International Joint Research Laboratory on Climate and Environment Change (ILCEC), Nanjing University of Information Science & Technology (NUIST), China*
[c] *Department of Meteorology, South Eastern Kenya University, Kitui, Kenya*

ABSTRACT: This study presents potential future variations of mean rainfall and temperature over East Africa (EA) based on five models that participated in the Coupled Model Intercomparison Project Phase 5 (CMIP5) and representative concentration pathways (RCPs): 4.5 and 8.5. In this study, climate simulations of two timeframes, a baseline period (1961–1990) and projection period (2071–2100), are compared. The models reproduce EA's bimodal rainfall pattern but overestimate and underestimate seasonal rainfall of October–December (OND) and March–May (MAM), respectively. Rainfall is projected to increase under the two scenarios. Larger increases in rainfall will occur during the OND season than during the MAM season and in RCP8.5 than in RCP4.5. During the last half of the 21st century, EA is likely to warm by 1.7–2.8 and 2.2–5.4 °C under the RCP4.5 and RCP8.5 scenarios, respectively, relative to the baseline period. Scenario uncertainty is projected to exceed model uncertainty from the middle to the end of the 21st century. The central parts of Kenya and the Lake Victoria Basin will witness the highest increases in seasonal rainfall. The probability density functions (PDFs) of future seasonal rainfall show a positive shift and a statistically insignificant increase in variance relative to the baseline. Thus, EA is likely to experience an increase in extreme rainfall events. Understanding the future climate variability in EA is important for planning purposes but these results are based on relatively course resolution models prone to bias and therefore should be used with caution. There is a need for further research on climate projections over EA, including determining the causes of the poor performance of global models in reproducing rainfall climatology and trends over the region.

KEY WORDS climate projection; rainfall; temperature; CMIP5; East Africa

Received 9 August 2016; Revised 18 July 2017; Accepted 26 July 2017

1. Introduction

Understanding ongoing and projected climate variability and change is essential for long-term planning at the global, regional, and local scales and is particularly important for countries/regions whose economies are heavily reliant on rain-dependent sectors. East Africa (EA; Kenya, Uganda, and Tanzania) is one such region and is highly vulnerable to the effects of climate variability and change (IPCC, 2007). This region's economy is strongly reliant on rain-fed agriculture (World Bank, 2008). Sustainable socioeconomic development in EA is paramount and requires making good use of available climate information to maximize agricultural productivity while protecting the environment. Consequently, the demands for research aimed at minimizing the uncertainties in climate projections are also growing. This study provides climate information for guiding the formulation and possible implementation of policies. One area that should be thoroughly researched is the vulnerability of agriculture to the effects of projected climate change. This research can be achieved by using available accurate and timely information regarding the expected changes in both mean and extreme climate events, which is still limited in EA (Omondi *et al.*, 2014; Ongoma *et al.*, 2016a).

Currently, general circulation model (GCM) simulations forced by specified variations in greenhouse gases (GHGs) are commonly used to understand future climate change. Although the performance of the models remains limited, the results from the models provide a qualitative guide for the expected climate (Knutti and Sedláček, 2013). The uncertainty in the models occurs for many reasons, including the accurate characterization of future GHG emissions. However, Jakob (2010) singled out simulations of moist, deep convection as the main source of uncertainty in model projections of the future climate over Africa and globally.

Rainfall is the most valuable weather parameter in EA (Muthama *et al.*, 2012), which explains why rainfall has been studied in more depth relative to other weather

* Correspondence to: V. Ongoma, International Joint Research Laboratory on Climate and Environment Change (ILCEC), Nanjing University of Information Science & Technology (NUIST), Ningliu Road 219, Nanjing 210044, China. E-mail: victor.ongoma@gmail.com

variables. Although temperature does not adversely affect many economic activities in the region, studies have shown that temperature has a strong influence on malaria cases, especially in highland areas. According to previous studies (Omumbo *et al.*, 2011; Stern *et al.*, 2011), the observed warming favours the survival of *Anopheles* mosquitoes that transmit malaria in EA. Thus, conducting investigations of the temperature change and variability in the region in future scenarios is worthwhile. A recent review study by Adhikari *et al.* (2015) that looked at the effects of climate change on agriculture and mainly focused on temperature over eastern Africa largely projected a negative impact of climate change on crop yields by the end of the 21st century. Understanding how climatic and non-climatic parameters will affect agricultural production in the region has prompted detailed studies of the projected variability of the most important weather parameters in EA.

Several studies (e.g. Ogallo, 1988; Indeje *et al.*, 2000; Black *et al.*, 2003; Oettli and Camberlin, 2005; Yang *et al.*, 2014, 2015a, 2015b; Gamoyo *et al.*, 2015; Nicholson, 2016; Schmocker *et al.*, 2016) focusing on rainfall variability have been conducted in EA. The ongoing variability of rainfall has led to increases in the intensities of drought and flood events (Anyah and Semazzi, 2006; Kijazi and Reason, 2009a, 2009b; Lyon and Dewitt, 2012; Lyon, 2014; Nicholson, 2016) associated with human and animal causalities and devastating economic losses. Notably, most extreme rainfall events that occur in the region are linked to El Niño-Southern Oscillation (ENSO) events (Ogallo, 1988; Indeje *et al.*, 2000). Current observations show that the region is experiencing high rainfall variability, with the main concern being the reduction in seasonal rainfall from March to May (MAM), although this reduction is statistically insignificant (Williams and Funk, 2011; Lyon and Dewitt, 2012; Maidment *et al.*, 2015; Tierney *et al.*, 2015). The seasonal rainfall during MAM has been given much attention because MAM is the main crop-growing season in EA; thus, excess or depressed seasonal rainfall during MAM results in food insecurity in the region. Although the performance of the Coupled Model Intercomparison Project Phase 5 (CMIP5) GCMs remains uncertain concerning rainfall projections (Kent *et al.*, 2015), most studies agree that the rainfall over the larger part of the Great Horn of Africa (GHA; Kenya, Uganda, Tanzania, Ethiopia, Rwanda, Burundi, Sudan, South Sudan, Eritrea, Djibouti, Somali) is likely to increase in the 21st century (Shongwe *et al.*, 2011; Christensen *et al.*, 2013; Tierney *et al.*, 2015). However, some individuals are against this generalization; Patricola and Cook (2011) projected negative rainfall anomalies in the months of August and September over Uganda and western Kenya. These authors attributed the decreasing rainfall to anomalous meridional moisture divergence. According to Yang *et al.* (2014, 2015b), the model projections of rainfall for EA should be treated with a lot of caution due to chronic biases of the models in simulation of the mean climate in the region and biases in simulating the tropical ocean responses to rising GHGs. This implies that the dry trend being observed might continue in the real world in contrast to the model projections.

Shongwe *et al.* (2011) using CMIP3 models, projected increases in both the mean rates and the intensity of high rainfall starting in the early 21st century. However, according to Nicholson (2014, 2016), the start of the upward trend of the rainfall as projected by Shongwe *et al.* (2011) has not been realized so far.

Anyah and Qiu (2012) investigated changes in rainfall and temperature over the GHA using 11 CMIP3 models. These authors projected equal and general increases in rainfall by the middle to the end of the 21st century during the four seasons and noted that the inter-annual variability of rainfall over the GHA is more likely to increase by the end of the 21st century. Furthermore, these authors reported that the minimum average surface temperature would increase by more than 2 °C by the end of the 21st century relative to the average minimum temperature between 1981 and 2000 under scenarios A1B and A2.

Otieno and Anyah (2013) used six CMIP5 model outputs to simulate climate conditions over the GHA under the RCP4.5 and RCP8.5 scenarios. According to their results, the tropical region is projected to experience greater rainfall from October to December (OND). In addition, the projected rainfall conditions are partially explained by the anomalous moisture influx from the Congo basin and Gulf of Guinea (Otieno and Anyah, 2013). The conclusion was based on the analysis of velocity potential, showing low level convergence over EA. In a different study, Segele *et al.* (2009) linked enhanced summer rainfall in Ethiopia to strengthened low-level westerlies over western and central Africa. The findings of that study agree with the observations made by Seneviratne *et al.* (2012), showing high confidence regarding the projected increase in heavy rainfall over the GHA. In IPCC AR5, Niang *et al.* (2014) observed that rainfall is likely to increase over EA although the projections remain uncertain. In an investigation of the changes of temperature and precipitation extremes over the GHA, Omondi *et al.* (2014) reported the likelihood of a greater number of warm days and nights and a lower number of cold nights in the future. These authors modelled the past and future climate over the GHA by using the PRECIS regional climate model (RCM).

Globally, the number of studies aimed at projecting regional climate is increasing. So far, few or no studies have been conducted that focus exclusively on rainfall and temperature projections over EA using the CMIP5 data set.

In this current study, CMIP5 GCM data are used to elaborate on the projected changes in mean annual and seasonal rainfall and temperature to answer the following question: 'How is the observed seasonal rainfall pattern in EA likely to change in the future under the projected warming climate based on CMIP5 models?' The outcomes of this study will provide an indication of how prone a region is to climate extremes, which is vital information for formulating measures to adapt to the climate change and variability projected to occur over EA. This

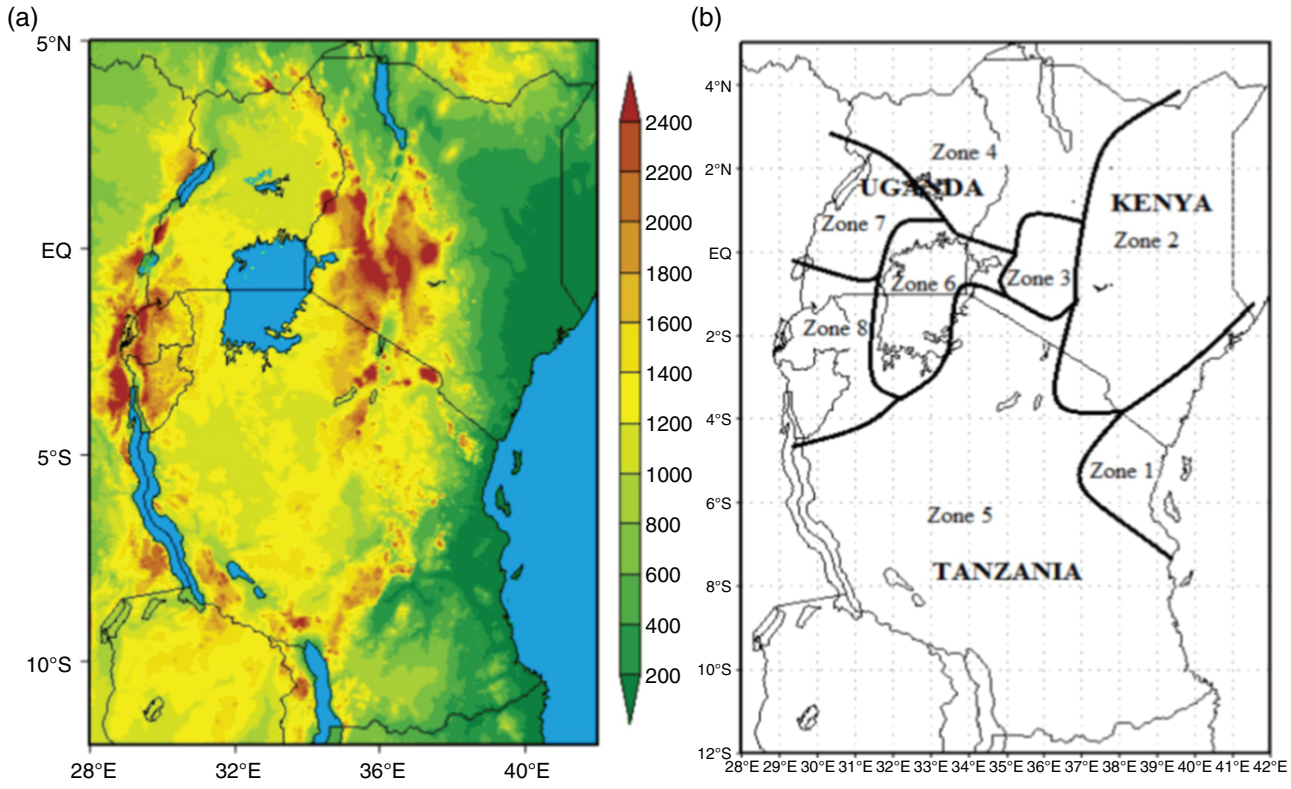

Figure 1. Topographical elevation map (metres) of East Africa. The three countries: UG – Uganda [29°E – 35°E, 1.5°S – 4°N], Kenya [35°E–41.5°E, 3°S–4.5°N], and Tanzania [29°E–40°E, 10°S–4°S].

study is limited to describing and quantifying climate changes and does not identify why the projected changes occur.

The rest of this work is divided into three main sections. Section 2 contains a brief description of the models as well as the methodology employed in the study. Section 3 presents the results and discussion, and Section 4 provides the conclusions and recommendations resulting from the study.

2. Data and methodology

2.1. Area of study

EA lies in the tropics within 28–42°E and 12°S–5°N (Figure 1). Although Rwanda and Burundi are part of the study area, they are geographically small relative to the other countries in the region and were thus regarded as part of Tanzania in this study.

The distribution of socioeconomic activity over EA is mainly influenced by rainfall, with most economic activities (e.g. production, manufacturing, and processing) being concentrated in zones of high rainfall. The rainfall in this region predominantly exhibits a bimodal pattern, with 'long rains' during MAM and 'short rains' during OND (Camberlin and Wairoto, 1997; Mutai and Ward, 2000; Camberlin and Philippon, 2002; Ongoma and Chen, 2017). The annual rainfall pattern is mainly influenced by the movement of the inter-tropical convergence zone (ITCZ) across the equator (Camberlin and Okoola, 2003; Yang *et al.*, 2015a). This region is characterized by rainfall that exhibits high spatial–temporal variability due to its varying topography and the presence of large water bodies (Indeje *et al.*, 2001; Oettli and Camberlin, 2005; Ogwang *et al.*, 2014). The variability of rainfall and common incidences of seasons with below and above normal rainfall (Hastenrath *et al.*, 2007) adversely impact food security and socioeconomic development in the region. The ENSO is the main factor that influences EA's inter-annual rainfall variability (Ogallo, 1988; Indeje *et al.*, 2000; Mutai and Ward, 2000). El Niño and La Niña events are associated with above and below normal rainfall in EA, which cause floods and droughts, respectively. As we enter the 21st century, the frequency and intensity of extreme rainfall events are likely to be intensified in EA (IPCC, 2007; Shongwe *et al.*, 2011), which, if not adapted to, will correspond with increasing socioeconomic losses.

Studies have shown that large-scale climatic factors have a greater influence on 'short rains' seasons than 'long rains' seasons. One good example of this effect is the influences of the Indian Ocean dipole (IOD) (Black *et al.*, 2003; Behera *et al.*, 2005; Manatsa *et al.*, 2012) and ENSO (Hastenrath *et al.*, 1993; Indeje *et al.*, 2000) on OND rainfall. By contrast, temperature experiences low spatiotemporal variability, with the highest temperature being recorded during the months of December until February and the lowest temperatures being recorded during the months of June until August.

The region is sub-divided into eight homogenous rainfall zones (Indeje *et al.*, 2000) (Table 1). Indeje

Table 1. The eight grid boxes representing homogenous rainfall zones over EA.

Region	Longitude	Latitude
R1	37.5–39°E	6–4°S
R2	37–40°E	2 S–2°N
R3	35–36.5°E	1°S–1°N
R4	32–36°E	2–4°N
R5	31–37°E	8–5°S
R6	31.5–33°E	3°S–0
R7	30–32°E	0–2°N
R8	30–31°E	4–1°S

et al. (2000) used an empirical orthogonal function (EOF) and other methods to map out a network of 136 stations over EA into homogeneous rainfall regions. The same zones were used in recent studies, including the studies of Ogwang (2015) and Shongwe *et al.* (2011).

2.2. Data

In this study, the multi-model ensemble (MME) simply abbreviated as ENSEM, mean of five models was used to project future rainfall. Data from 1900 to 2100 were sourced from five (Table 2) of the top eight World Climate Research Program (WCRP) CMIP5 models selected in an earlier study by Ongoma *et al.* (2016b). The five models were selected from the top eight models based on data availability. The CMIP5 data are archived and are made freely available by the Program for Climate Model Diagnosis and Intercomparison (PCMDI) at http://pcmdi3.llnl.gov/esgcet/home.htm. In this study, CMIP5 gridded climate data at a horizontal resolution of 1° by 1° were sourced from Canadian climate data and scenarios (http://www.cccsn.ec.gc.ca).

The CMIP5 models are driven by a new set of atmospheric composition forcings – the 'historical forcing' for current climate conditions and RCPs for future scenarios (Moss *et al.*, 2010; Hibbard *et al.*, 2011; Taylor *et al.*, 2012). These scenarios provide a picture of how the future climate will respond to the ongoing increase of GHG concentrations in the atmosphere. Table 3 provides the following RCPs that are considered in this study: RCP4.5 and RCP8.5.

Monthly reanalysed rainfall data sourced from Climate Research Unit (CRU) was used to assess the performance of CMIP5 models in reproducing rainfall climatology over EA. The CRU TS3.22 is discussed at length by University of East Anglia Climatic Research Unit (2014).

2.3. Methodology

2.3.1. The spatial patterns of rainfall anomalies over EA

The transient climate change scenarios for the five GCMs were generated by computing the anomalies between two periods: a baseline period from 1961 to 1990 and a future period from 2051 to 2100. The baseline period adopted in this study is the 30-year 'normal' period based on the definition provided by the World Meteorological Organization (WMO) (IPCC, 2001).

An analysis of decadal rainfall change was carried out to detect rainfall anomalies. The future rainfall was categorized into five decades: 2051–2060, 2061–2070, 2071–2080, 2081–2090, and 2091–2100. The future climate change was computed as the differences in rainfall between the future period (2071–2100) under the RCP4.5 and RCP8.5 scenarios and the baseline period (1961–1990).

2.3.2. Time series analysis

A trend analysis for rainfall was carried out using the Mann–Kendall (MK) test statistic. The MK test is a nonparametric rank-based test used to determine the nature of the trend of a given time series against the null hypothesis of no trend (Mann, 1945; Kendall, 1975). The application of this method is becoming common in environmental and hydrological studies in EA (Ongoma *et al.*, 2013; Nsubuga *et al.*, 2014a, 2014b; Ongoma and Chen, 2017).

The Theil–Sen's slope estimator (Theil, 1950; Sen, 1968) was used to measure and compare the magnitude of rainfall change in different homogeneous rainfall zones over EA. This method is a nonparametric approach that can be used to estimate the magnitudes of decreasing or increasing trends. When using this method, the estimated slope provides a median value for all possible combinations of pairs for the entire data set. Positive values denote an increasing trend whereas negative values denote a downward slope.

2.3.3. Probability density function (PDF)

PDFs are calculated for the baseline period and future annual and seasonal rainfall to show how the MME dispersion is projected to change under the RCP4.5 and RCP8.5 scenarios. The PDFs show the changes of the mean and variance of rainfall during the periods under study. The probability was calculated using kernel density estimation (KDE), with a biweight kernel to design PDFs that were a better fit for EA owing to the high spatiotemporal variability of rainfall in the region. KDE is a nonparametric approach that can be used for estimating PDFs as discussed by Bernacchia and Pigolotti (2011).

F-test statistic is used to examine the variances between the rainfall in the baseline period and the projection periods, according to Snedecor and Cochran (1989). The significance was tested at 5% significant level.

3. Results and discussion

3.1. Rainfall climatology

Figure 2 shows the annual rainfall cycle over EA for the model simulations of the baseline period. GCMs adequately capture the expected bimodal pattern of rainfall. However, similar to the observations made in

Table 2. The CMIP5 modelling centres, model names, and their respective horizontal resolutions used in this study.

Modelling centre	Model name	Horizontal resolution (lon × lat)
1 Canadian Centre for Climate Modelling and Analysis (Canada)	CanESM2	~2.81°× 2.79°
2 Community Earth System Model Contributors (United States)	CESM1-CAM5	1.25 × 0.942°
3 Centre National de Recherches Météorologiques (France)	CNRM-CM5	~1.406 × 1.401°
4 Commonwealth Scientific and Industrial Research Organization (Australia)	CSIRO-Mk3.6.0	~1.875 × 1.865°
5 Atmosphere and Ocean Research Institute (The University of Tokyo), National Institute for Environmental Studies, and Japan Agency for Marine–Earth Science and Technology (MIROC) (Japan)	MIROC5	~1.406 × 1.401°

Table 3. RCPs considered in this study.

RCP	Forcing
RCP4.5	Stabilization scenario whereby the total radiative forcing is stabilized shortly after 2100. This will be achieved by adopting several technologies and strategies to cut GHG emissions (Thomson *et al.*, 2011)
RCP8.5	This is 'business-as-usual' scenario. It is characterized by rising radiative forcing pathway leading to 8.5 W m^{-2} by 2100, with forcing increasing further thereafter up to 12 W m^{-2} by 2250, when concentrations stabilize (Riahi *et al.*, 2011)

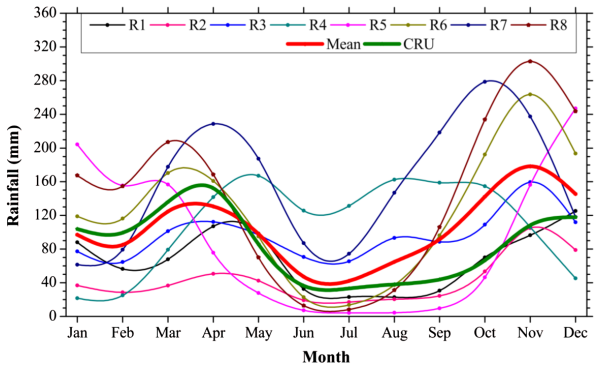

Figure 2. The annual rainfall cycle (mm) over the EA homogeneous rainfall zones based on the CMIP5 mean ensemble data for the period 1961–1990. The thick green (red) line shows the mean rainfall over EA based on model (CRU) data. R1–R8 represent regions 1–8, respectively. [Colour figure can be viewed at wileyonlinelibrary.com].

Table 4. Summary of the MK test statistic for seasonal rainfall during MAM and OND over EA for the period of 2071–2100 at the 5% significance level.

	MAM		OND	
	RCP4.5	RCP8.5	RCP4.5	RCP8.5
S	−19	53	−31	107
Z	0.031	0.928	0.535	1.891
p	0.748	0.354	0.592	0.057
Significance	Insignificant	Insignificant	Insignificant	Insignificant

S_{and} Z_{are} MK test statistic and standardized test statistic, respectively.

previous studies (Anyah and Qiu, 2012; Yang *et al.*, 2015a; Klein *et al.*, 2016; Ongoma *et al.*, 2016b), the CMIP models tend to underestimate and overestimate seasonal rainfall during MAM and OND, respectively. According to Yang *et al.* (2015b), the observed bias in 'long' and 'short' rains is linked to problems in simulating the atmosphere–ocean–monsoon interaction over the EA–Indian Ocean–Asian monsoon. The models capture the annual cycle of rainfall in all regions fairly well. For instance, the main rainfall season in R5 was from November to February, coinciding with summer in the Southern Hemisphere, which was expected (Owiti and Zhu, 2012). Conversely, R3 exhibits a trimodal rainfall pattern, with the third season occurring in June–August (Mutai *et al.*, 1998; Indeje *et al.*, 2000). Indeje *et al.* (2000) noted that the rainfall in June until August extends into September in some parts of Africa and is mainly confined to the western highlands of Kenya and a large portion of Uganda. The western highlands of Kenya extending into Uganda correspond to R3 and R4 in this study. Regarding the amounts of rainfall, R1 and R2 correspond with the lowest amounts of rainfall and R7 and R8 correspond with the highest amounts of rainfall throughout the year. The areas classified as R7 consist of arid and semi-arid land (ASAL) whereas the areas classified as R8 benefit from the influx of moisture from the Atlantic Ocean and Congo basin. The equatorial westerlies flowing from Atlantic Ocean through Congo basin are known to be unstable

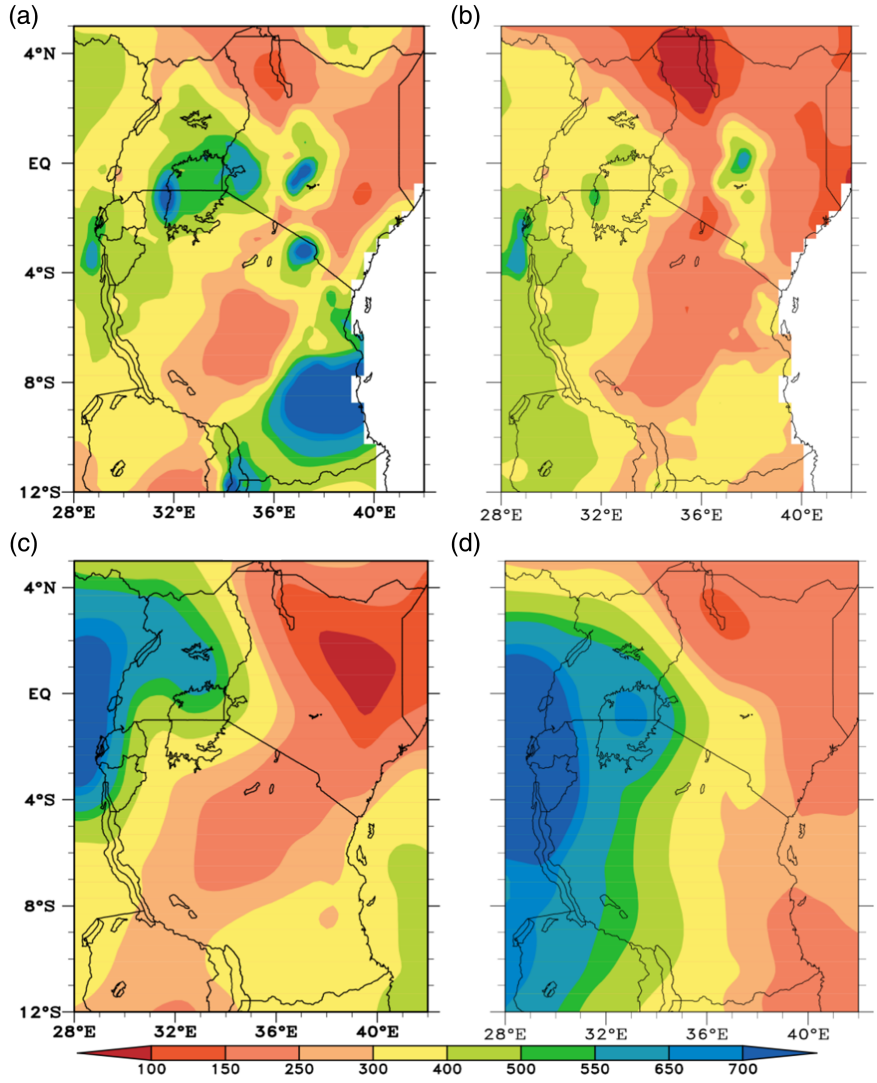

Figure 3. Seasonal rainfall (mm) over EA based on CRU data set (top), and CMIP5 models (bottom) for the period 1961–1990; March–May (left), and October–December (right). [Colour figure can be viewed at wileyonlinelibrary.com].

and moist, and are linked to wet spells in EA (Okoola, 1999). Camberlin and Philippon (2002) found westerly winds from the Congo basin to be one of the satisfactory predictors of MAM rainfall over EA.

Maps of the modelled seasonal rainfall climatology for the period 1961–1990 over EA are presented in Figure 3. The maximum rainfall occurs over the western parts of the study area and decrease eastward. Similarly, Kizza *et al.* (2009) observed that the mean annual rainfall within the basin ranged from 2037 mm in Bukoba to 847 mm in Musoma. The small amounts of rainfall in the northeastern parts of the study area and in central Tanzania are expected because the zones in this region are classified as ASAL (Indeje *et al.*, 2000). In observations, the amount, coverage, and period of rainfall during MAM are greater than those during OND, which explains why these seasons are referred to as 'long' and 'short' rainy seasons, respectively (Camberlin and Philippon, 2002). However, the seasonal distribution of modelled rainfall (Figure 3) shows that the amount is higher during OND than during MAM. That is, the CMIP3/5 models overestimate 'short rains' and underestimate 'long rains' as noted in previous studies (Anyah and Qiu, 2012; Yang *et al.*, 2015a, 2015b).

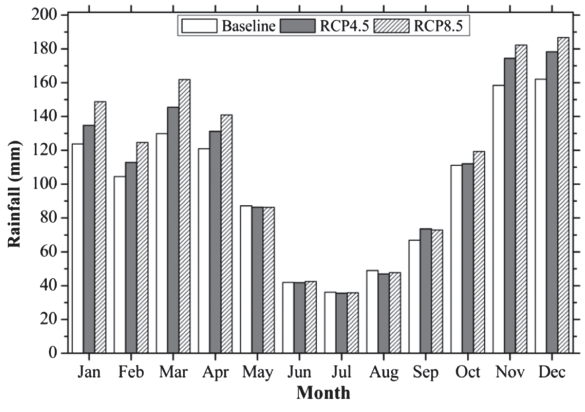

Figure 4. Monthly modelled rainfall climatology (mm) for the period of 1961–1990 and for the projected period of 2071–2100 (mm) over EA under the RCP4.5 and 8.5 scenarios.

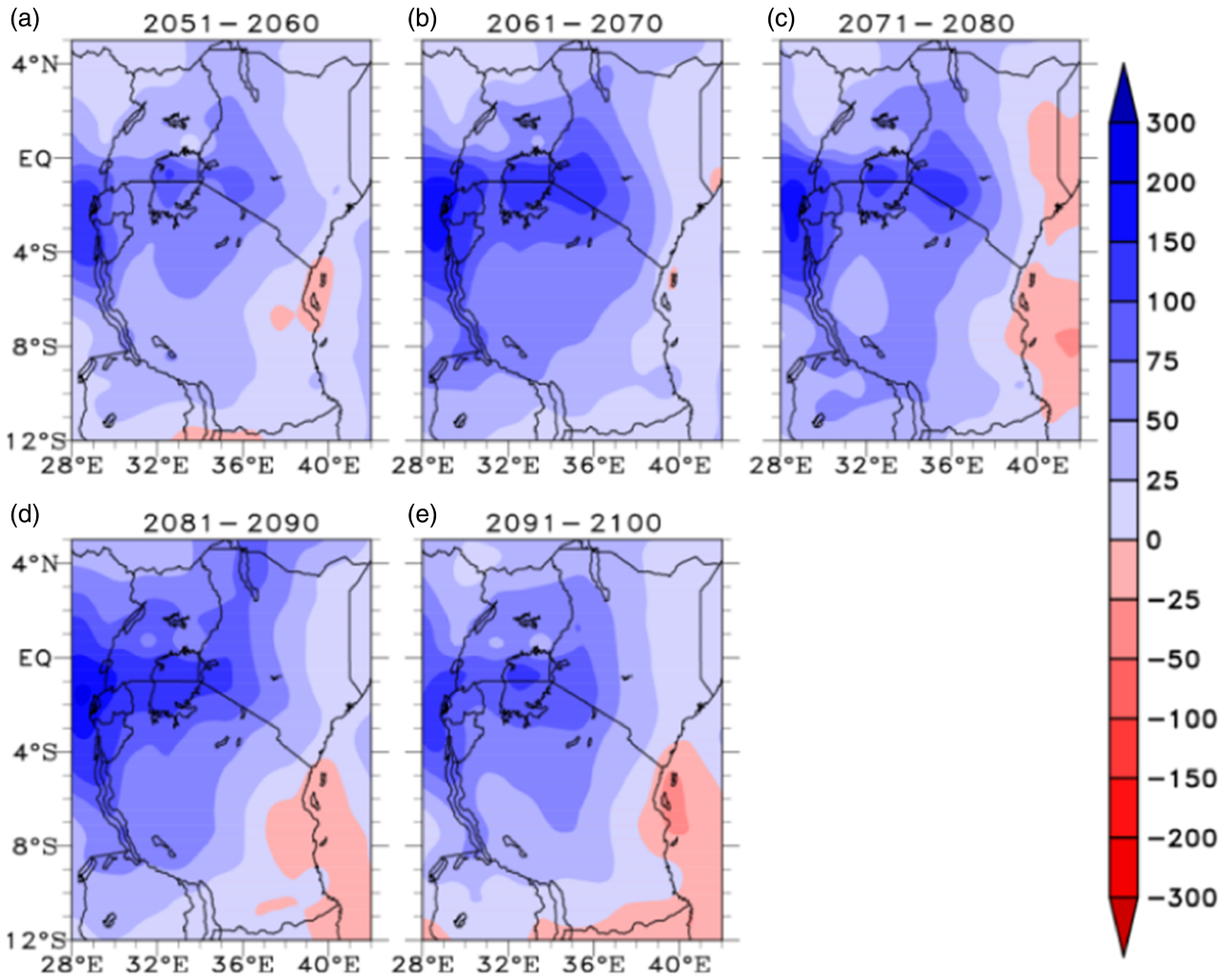

Figure 5. Decadal MAM rainfall change (mm) over EA based on the five CMIP5 ENSEM mean under the RCP4.5 scenario, relative to the baseline period 1961–1990. [Colour figure can be viewed at wileyonlinelibrary.com].

3.2. Spatiotemporal variability of projected rainfall

The projected increases of rainfall over the entire region of EA are higher during OND than during MAM, under the two scenarios. The positive changes in rainfall are insignificant at the 5% significance level during both seasons (Table 4). The insignificant trend in the MAM season reduces the significance of the annual rainfall because the MAM seasonal rainfall has a higher overall contribution to the annual rainfall than the OND seasonal rainfall.

Figure 4 gives the monthly changes of rainfall in the future, relative to the baseline data. Wet conditions are projected to occur over EA between September and April. The months of May to August are likely to witness a reduction in wet conditions. These results are in close agreement with Patricola and Cook (2011), who projected severe drying over southern Sudan and Uganda would occur in the months August of September. These authors attributed this projection to the weakening of the Somali jet stream and Indian monsoon. According to Segele *et al.* (2009), a strong Somali jet stream is associated with enhanced rainfall (above normal) over the Horn of Africa. The projected reduction in rainfall during these months is also partly explained by a reduction in evaporation (Patricola and Cook, 2011).

As shown in Figure 4, the projected wetting under RCP8.5 is greater than under RCP4.5. Notably, March has the highest rate of projected increased rainfall, which is favourable for farming because the month coincides with the start of the planting season in EA. At the seasonal level, the overall increase in rainfall during MAM, should it occur, will be a return to wetter conditions considering the reduction in rainfall during MAM over the GHA in recent decades (Lyon and Dewitt, 2012; Williams *et al.*, 2012; Liebmann *et al.*, 2014; Yang *et al.*, 2014; Maidment *et al.*, 2015; Schmocker *et al.*, 2016).

Figures 5–8 show ensemble-averaged seasonal rainfall projections for 2051–2100 under the RCP4.5 and RCP8.5 scenarios. Most parts of the study area will experience a positive change in rainfall, with greater changes occurring during OND than during MAM in all decades and scenarios. Similarly, the areas covering

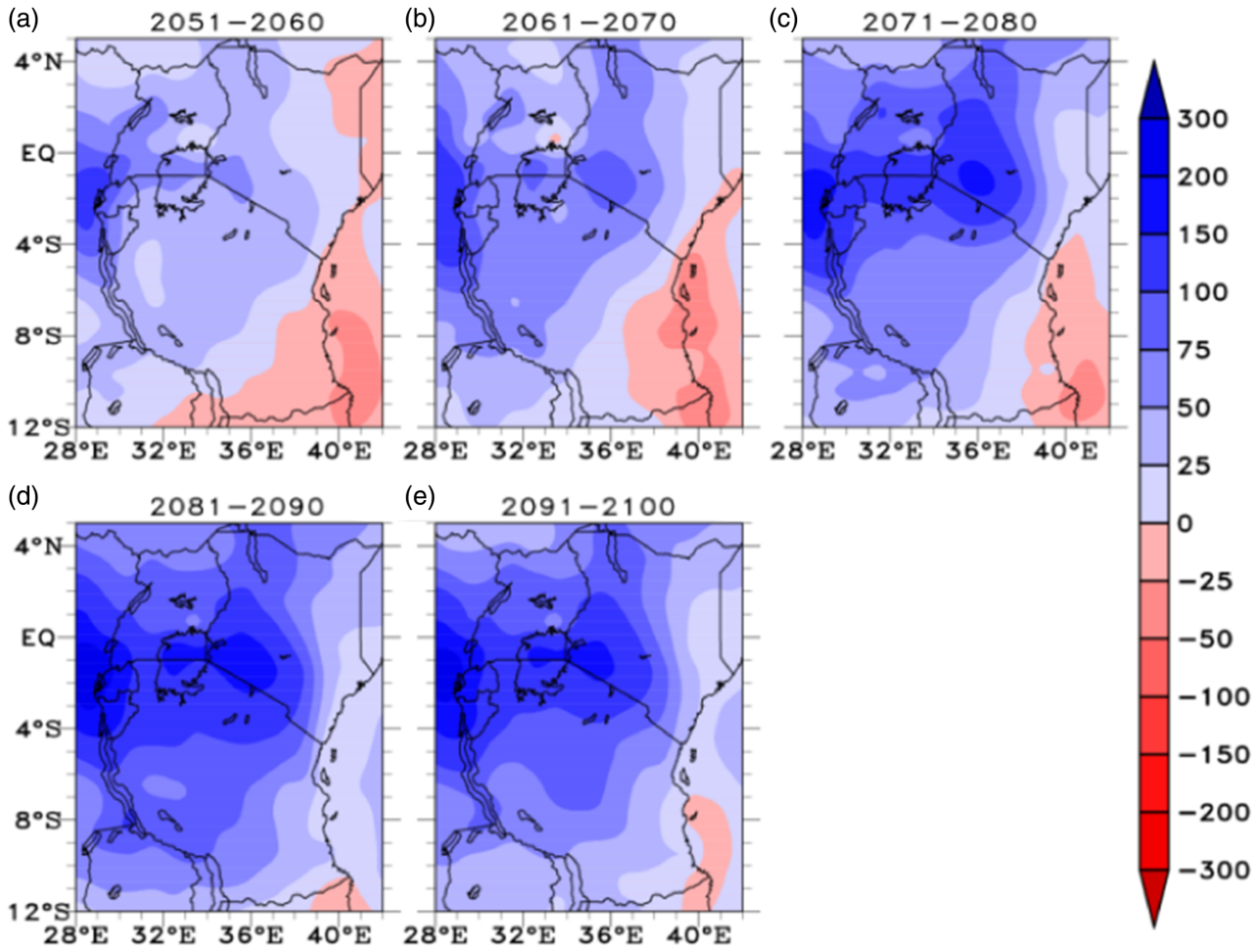

Figure 6. Decadal MAM rainfall change (mm) over EA based on the five CMIP5 ENSEM mean under the RCP8.5 scenario, relative to the baseline period 1961–1990. [Colour figure can be viewed at wileyonlinelibrary.com].

Kenya and northern Tanzania will record the highest increases in rainfall. Shongwe *et al.* (2011) linked the projected wetness during OND to higher warming rates over the western Indian Ocean than over the eastern Indian Ocean, increasing the chances of positive IOD occurrence.

Under the RCP4.5 scenario, the highest amount of wetting is projected to occur in the 2080s (Figures 5 and 7) with reduction in rainfall during the 2090s resulting from the stabilization of total radiative forcing before 2100 in the RCP4.5 scenario. Under RCP8.5, both rainfall seasons have rainfall increasing over the entire century.

Time series of annual rainfall over homogeneous rainfall zones over EA from 1961 to 2100 are presented in Figure 9. The magnitude of the slopes of the annual rainfall for the period of 2006–2100 over the homogeneous rainfall zones in EA (Figure 9) are presented in Table 5. The rainfall is projected to increase in all zones, with the increase under RCP8.5 being greater than that under RCP4.5. Generally, R3 and R8 will experience the highest rates of rainfall increase, whereas R1 and R4 will experience the lowest change of rainfall with time.

3.3. Rainfall PDFs

The PDFs for annual and seasonal rainfall over EA in the baseline period and RCP4.5 and RCP8.5 scenarios are displayed in Figure 10. The rainfall is projected to increase although the changes in variance are statistically insignificant at 5% significant level, except for RCP8.5 scenario during OND. The projected increase in annual and seasonal rainfall increases the likelihood of flooding and the reduced likelihood of drought in EA and the GHA, consistent with Shongwe *et al.* (2011), who used the earlier CMIP3 GCMs.

Figures 11 and 12 present the PDFs of mean rainfall over homogeneous rainfall regions for MAM and OND, respectively. For each region with an exception of R7 for MAM season under RCP4.5, rainfall increases from the baseline period to the RCP4.5 scenario and then to the RCP8.5 scenario. In MAM, the largest positive shift in mean rainfall will occur in regions 1–3 implying that the ASAL will become wet at a faster rate than the other parts of the study area. However, significant change in rainfall variance at 5% significant level will only be realized in R2. The OND season has a similar pattern of projected rainfall change, but the number of regions that will likely

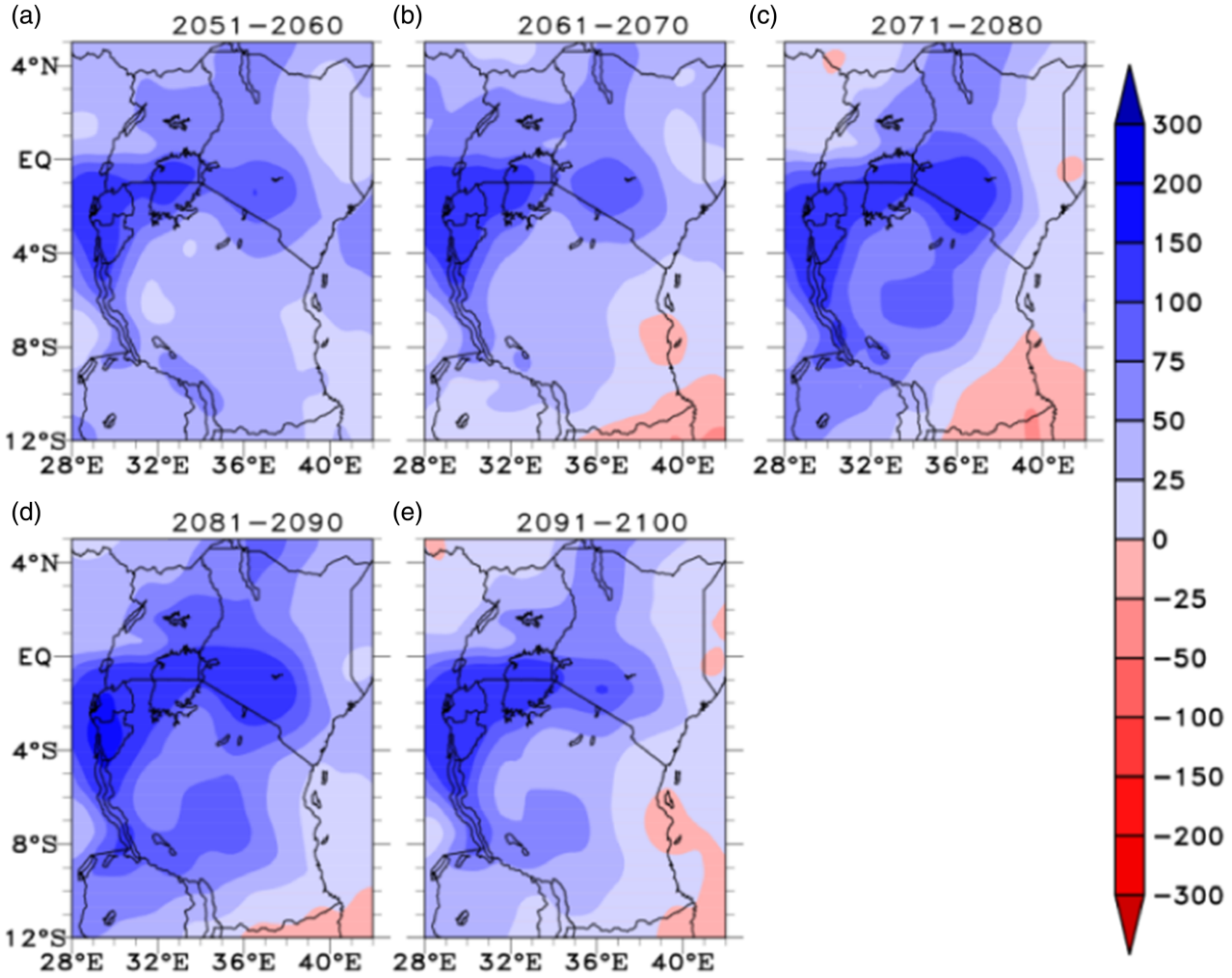

Figure 7. Decadal OND rainfall change (mm) over EA based on the five CMIP5 ENSEM mean under the RCP4.5 scenario, relative to the baseline period 1961–1990. [Colour figure can be viewed at wileyonlinelibrary.com].

record more rainfall in the two scenarios will be higher than during MAM. However, no region will observe a significant change in variance of rainfall at 5% significant level. Generally, the shift in mean rainfall towards the positive tail is larger in almost all regions during OND than during MAM.

3.4. Past and projected temperature over EA

The temperatures over EA based on the CMIP5 model ensemble mean for 1961–1990 are presented in Figure 13. The highest temperatures, which exceed 25 °C, are in northern and eastern Kenya, extending to eastern Tanzania. These regions are mainly within ASALs, which explains the relatively high temperatures. The lowest temperatures are in the mountainous areas, which agree with the observations made by Ogwang *et al.* (2014) that rainfall (temperature) decreases (increases) as the elevation decreases over EA. On average, the mean temperature for the period of 2006–2100 under the RCP8.5 scenario will be 25.3 °C, whereas the mean temperature will be 24.5 °C under the RCP4.5 scenario (Table 6).

Figure 14 presents the density functions of the baseline period (1961–1990) and projected (2071–2100) temperature over EA and shows that the mean temperature will be 25.2 and 26.7 °C under the RCP4.5 and RCP8.5 scenarios, respectively. Relative to the climatological mean, the projected temperature increases by approximately 2.4 and 4.1 °C under the RCP4.5 and RCP8.5 scenarios, respectively. This figure also indicates that the variance of the temperature increases remarkably from RCP4.5 to RCP8.5. The variance is generally high, calling for verification studies of these results using high resolution data sets.

Figure 15 shows the temperature projections over EA under RCP4.5 and RCP8.5. The simulations under the RCP8.5 scenario show consistent temperature increases throughout the projection period. Under the RCP4.5 scenario, the warming trend slows down beginning in the middle of the 21st century. By the end of the 21st century, the highest temperature that will be reached under the RCP4.5 scenario is nearly the same as the lowest temperature that will be recorded under the RCP8.5 scenario. Figure 15 shows that the spread of the models from the mean,

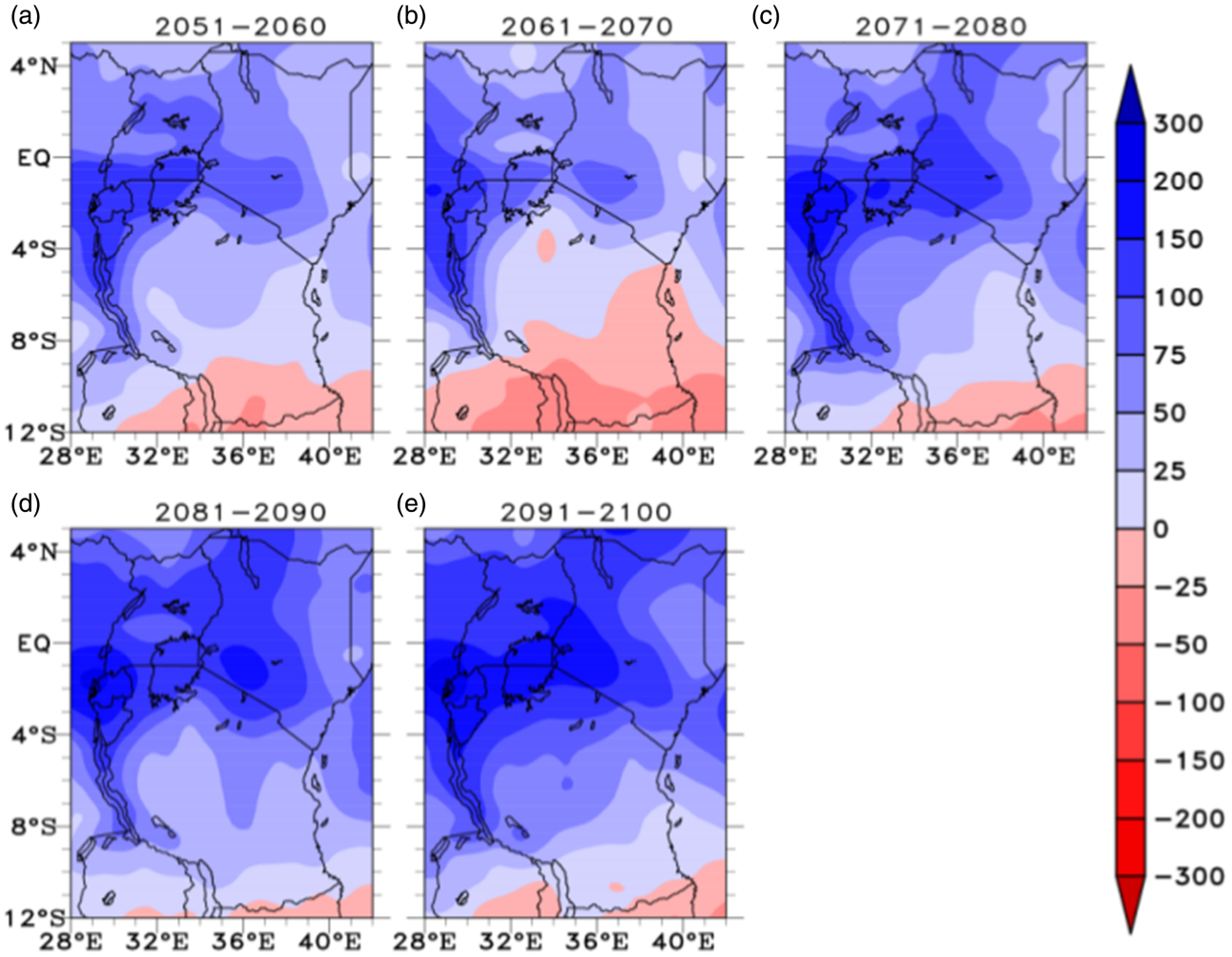

Figure 8. Decadal OND rainfall change (mm) over EA based on the five CMIP5 ENSEM mean under the RCP8.5 scenario, relative to the baseline period 1961–1990. [Colour figure can be viewed at wileyonlinelibrary.com].

especially under the RCP8.5 scenario, increases with time. Scenario uncertainty is evident from the middle of the 21st century onwards, when the temperature under the RCP8.5 scenario continues to increase whereas the trend under the RCP4.5 scenario becomes stable. Overall, the scenario uncertainty is dominant over the model uncertainty from the middle to the end of the 21st century, as observed by Hawkins and Sutton (2009, 2011).

Considering the entire climate projection period of 2006–2100, the results show that the temperature is likely to increase at 0.2 and 0.5 °C decade^{-1} under RCP4.5 and RCP8.5, respectively (Table 6). This result closely corroborates the earlier findings of Otieno and Anyah (2013), who considered a relatively larger area than EA. According to their study, the temperatures over the southern and equatorial GHA will likely increase at a rate of 0.3 and 0.4 °C decade^{-1} under the RCP4.5 and RCP8.5 scenarios, respectively, by the middle of the 21st century. If this extent of temperature increase is reached, it will be higher than the increase observed during the warming period from the end of the 20th century to the beginning of the 21st century, as reported by Camberlin (2017). According to Camberlin (2017), evidence indicates that warming occurred between 1973 and 2013 over the GHA, with minimum temperature increases of 0.20–0.25 °C decade^{-1} depending on season, and maximum temperature increases of 0.17–0.22 °C decade^{-1}.

Figures 16 and 17 show the mean temperature changes projected by the CMIP5 model ensemble for the 2050s, 2060s, 2070s, 2080s, and 2090s relative to the climatological period (1961–1990) under the two RCP scenarios. Under the RCP4.5 scenario, the mean warming over EA during the last half of the 21st century is likely to range between 1.7 and 2.8 °C. In the 'business as usual' scenario, the warming is likely to range between 2.2 and 5.4 °C. In both scenarios, the highest warming will be in central to western Tanzania and northern Kenya, and the smallest change will be along the coast of the Indian Ocean. These observations are in agreement with those of Engelbrecht *et al.* (2015), who reported that the temperature is likely to increase by 3–5 °C in the African tropics during 2071–2100 relative to 1961–1990 under the high emission scenario. Similarly, Dike *et al.* (2015) projected temperature increase within the African tropics, varying

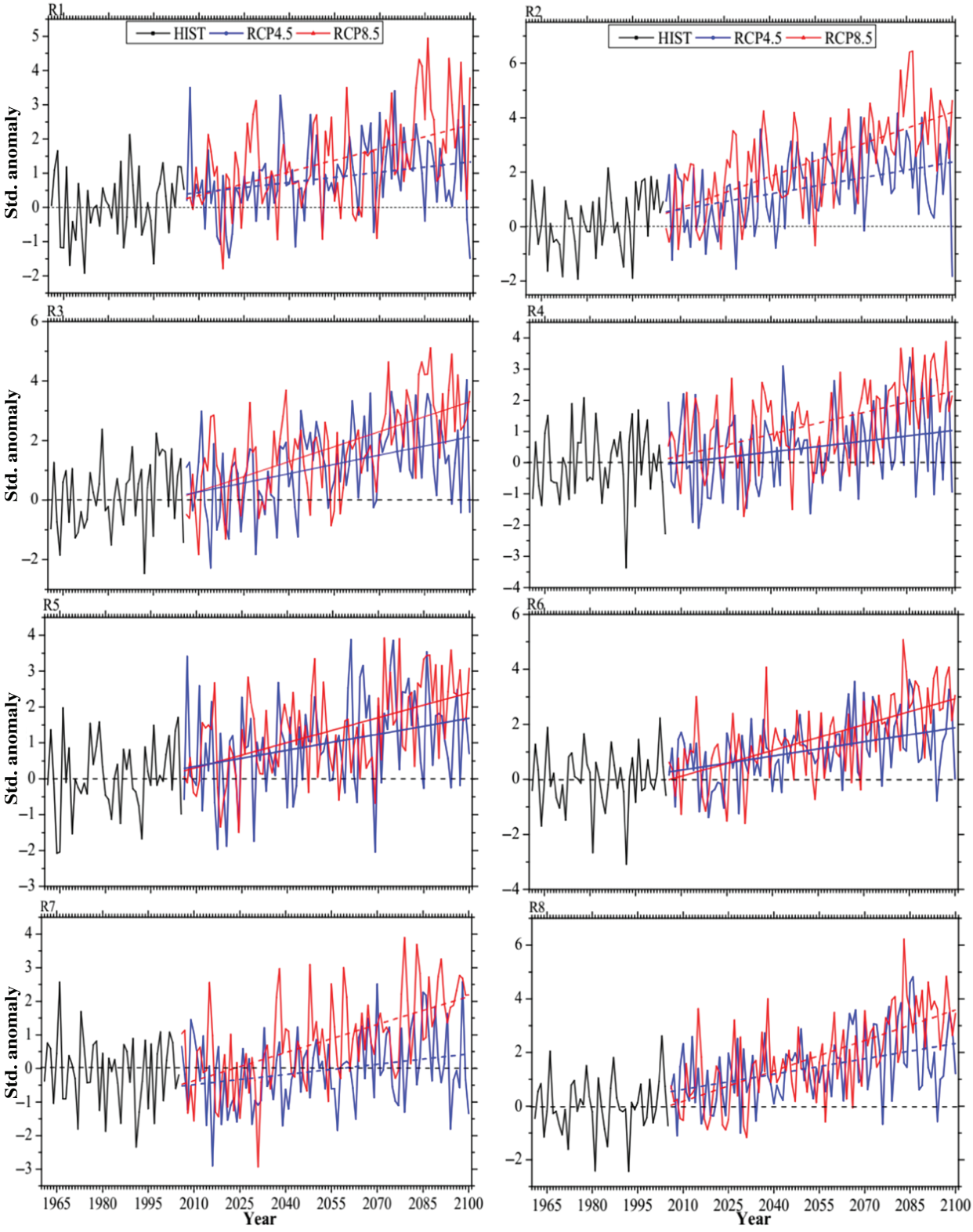

Figure 9. Rainfall anomaly over homogeneous rainfall zones in EA under the RCP4.5 and 8.5 scenarios for 1961–2100 (HIST represents the historical period of 1961–2005). R1–R8 represent regions 1–8, respectively.

from 3 to 7 °C for the period 2073–2098. The global temperature is projected to increase by 3 °C (IPCC, 2007; Niang *et al.*, 2014), which implies that the projected warming over EA is approximately 1.5 times the global warming projection.

4. Conclusion

Although EA does not experience high spatiotemporal variability in temperature given that it is located in the tropics, the significant change in temperature is likely to affect socioeconomic activities, such as agriculture and

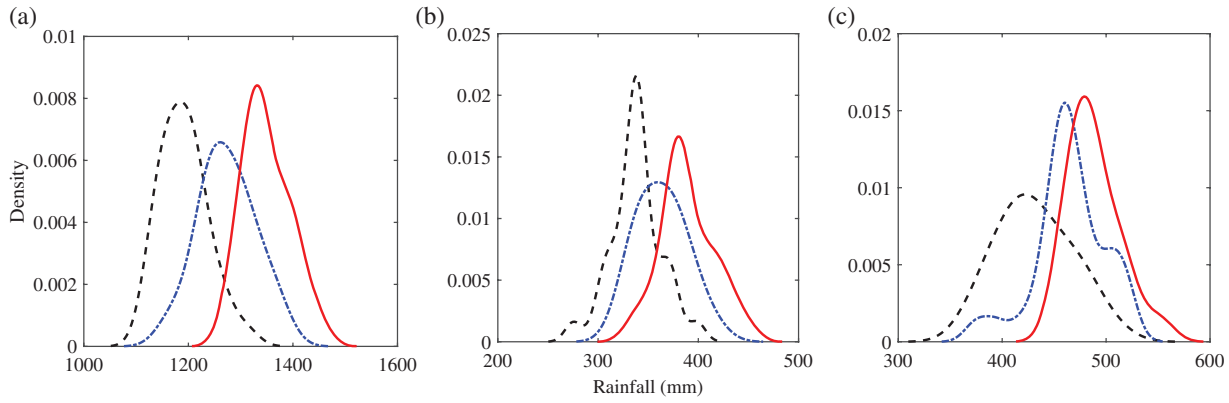

Figure 10. PDFs for rainfall distribution, (a) annual, (b) MAM, and (c) OND, under different RCP scenarios for EA [RCP4.5 (blue) and RCP8.5 (red) scenarios] for 2071–2100 and baseline period [1961–1990 (black)].

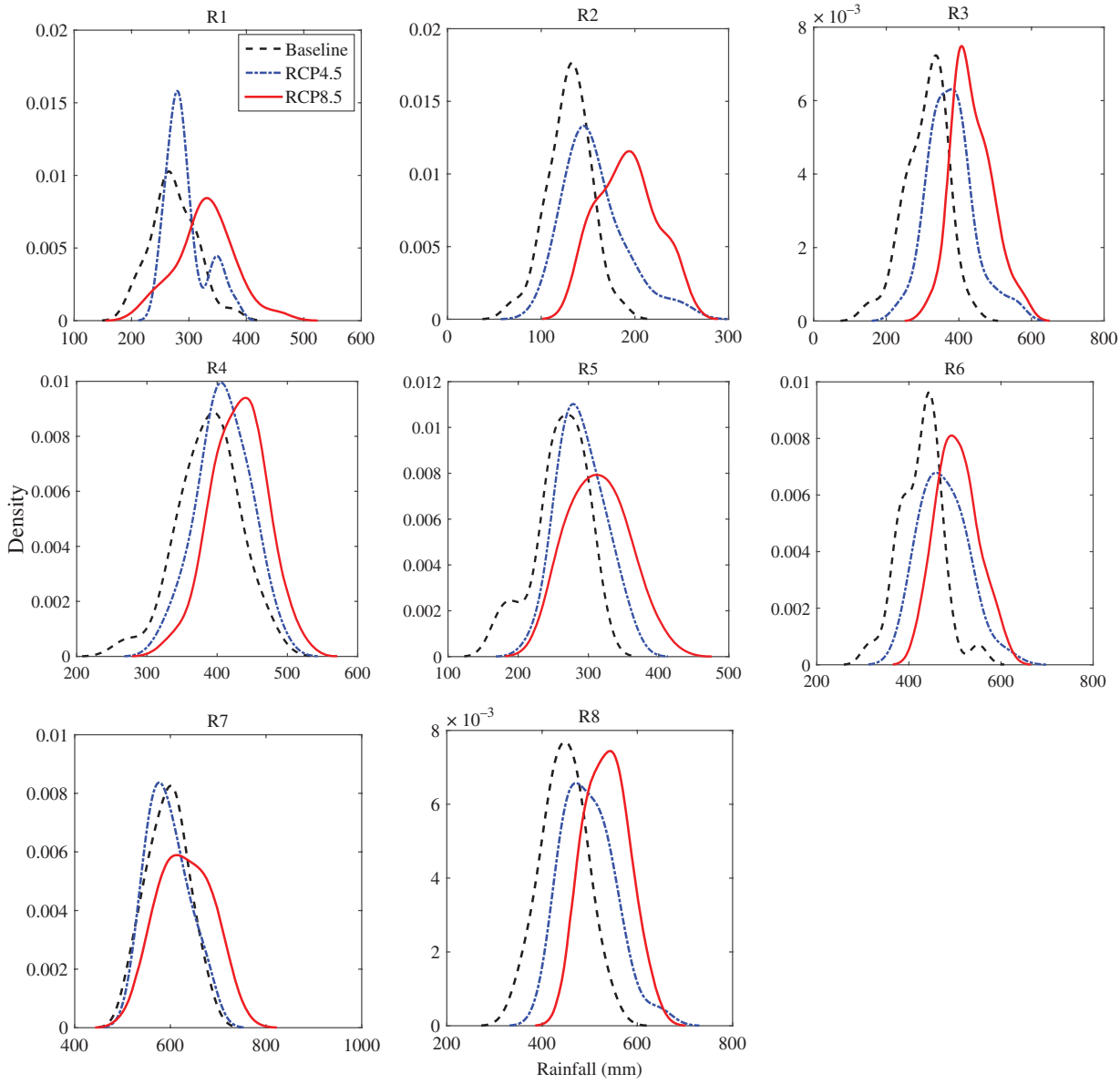

Figure 11. PDFs for seasonal rainfall during MAM seasonal under different RCP scenarios for EA [for the RCP4.5 (blue) and RCP8.5 (red) scenarios] for 2071–2100 and baseline period [1961–1990 (black)]. R1–R8 represent regions 1–8, respectively.

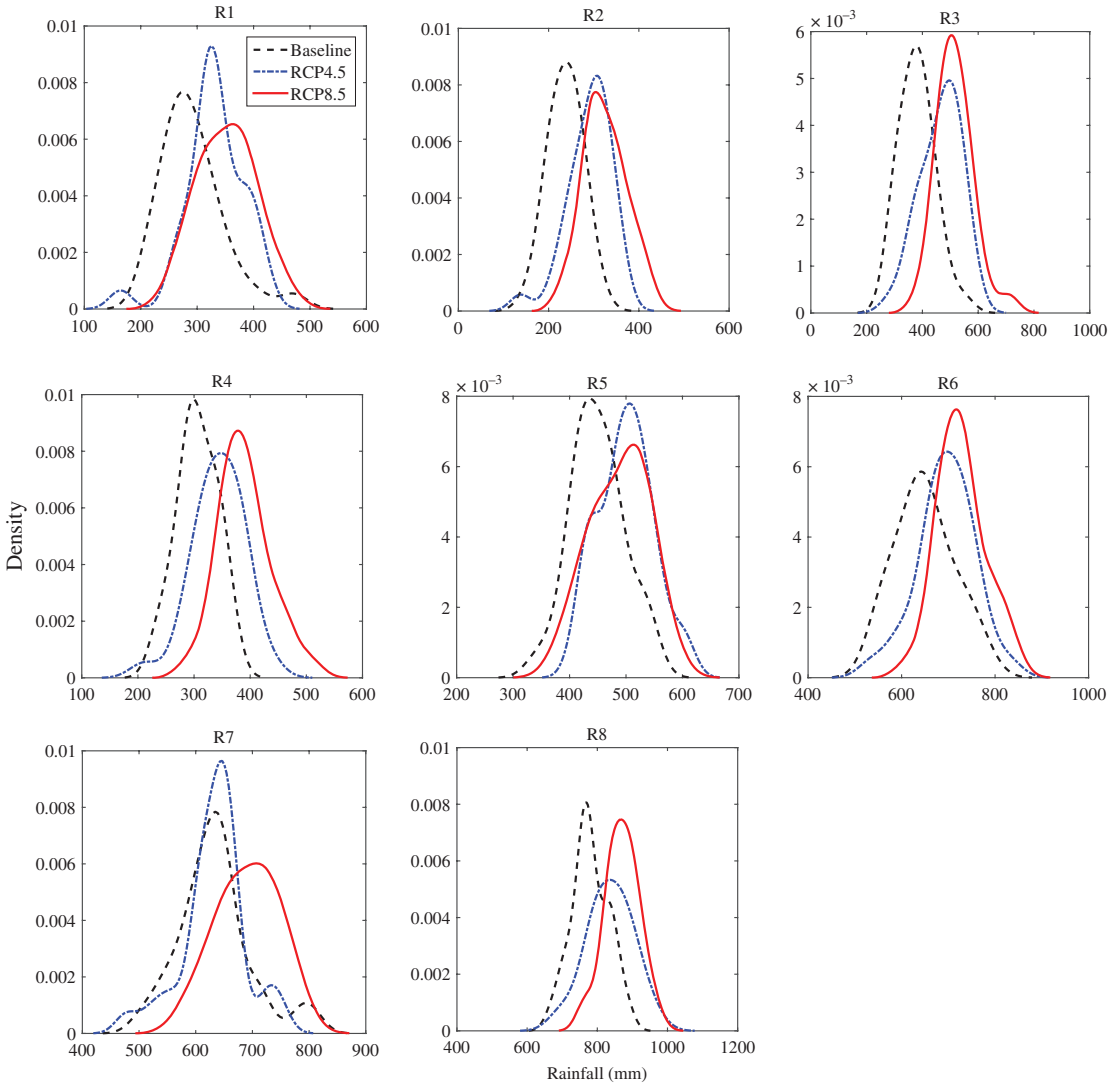

Figure 12. PDFs for the seasonal rainfall distribution during OND under different RCP scenarios for EA [for RCP4.5 (blue) and 8.5 (red) scenarios] for 2071–2100 and baseline period [1961–1990 (black)]. R1–R8 represent regions 1–8, respectively.

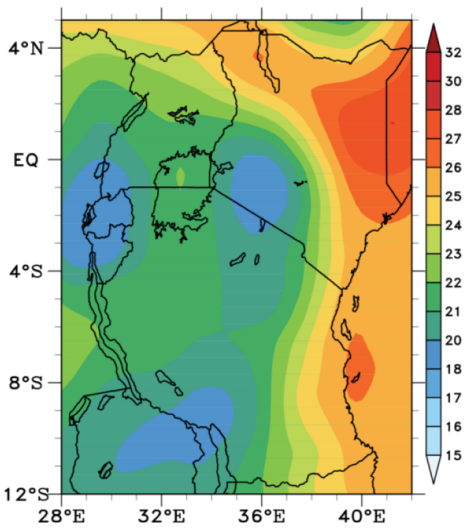

Figure 13. Temperatures (°C) over EA based on the CMIP5 model ensemble mean for 1961–1900.

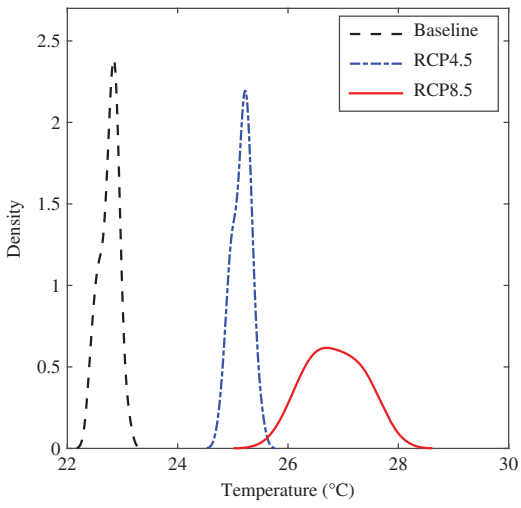

Figure 14. PDFs for the annual temperature distributions under different RCP scenarios for EA [for the RCP4.5 (blue) and 8.5 (red) scenarios] for 2071–2100 and to baseline period [1961–2000 (black)].

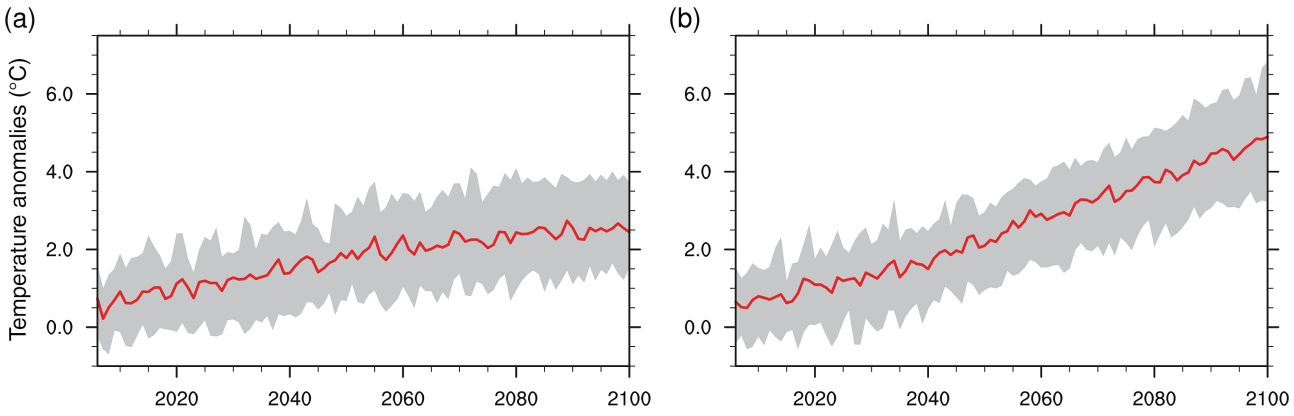

Figure 15. Standard anomaly of annual temperature projections over EA relative to the baseline period. This figure shows the temperature evolution under the (a) RCP4.5 and (b) RCP8.5 scenarios. The red lines correspond to the multi-model averages whereas the grey shaded areas show the temperature range in the individual models.

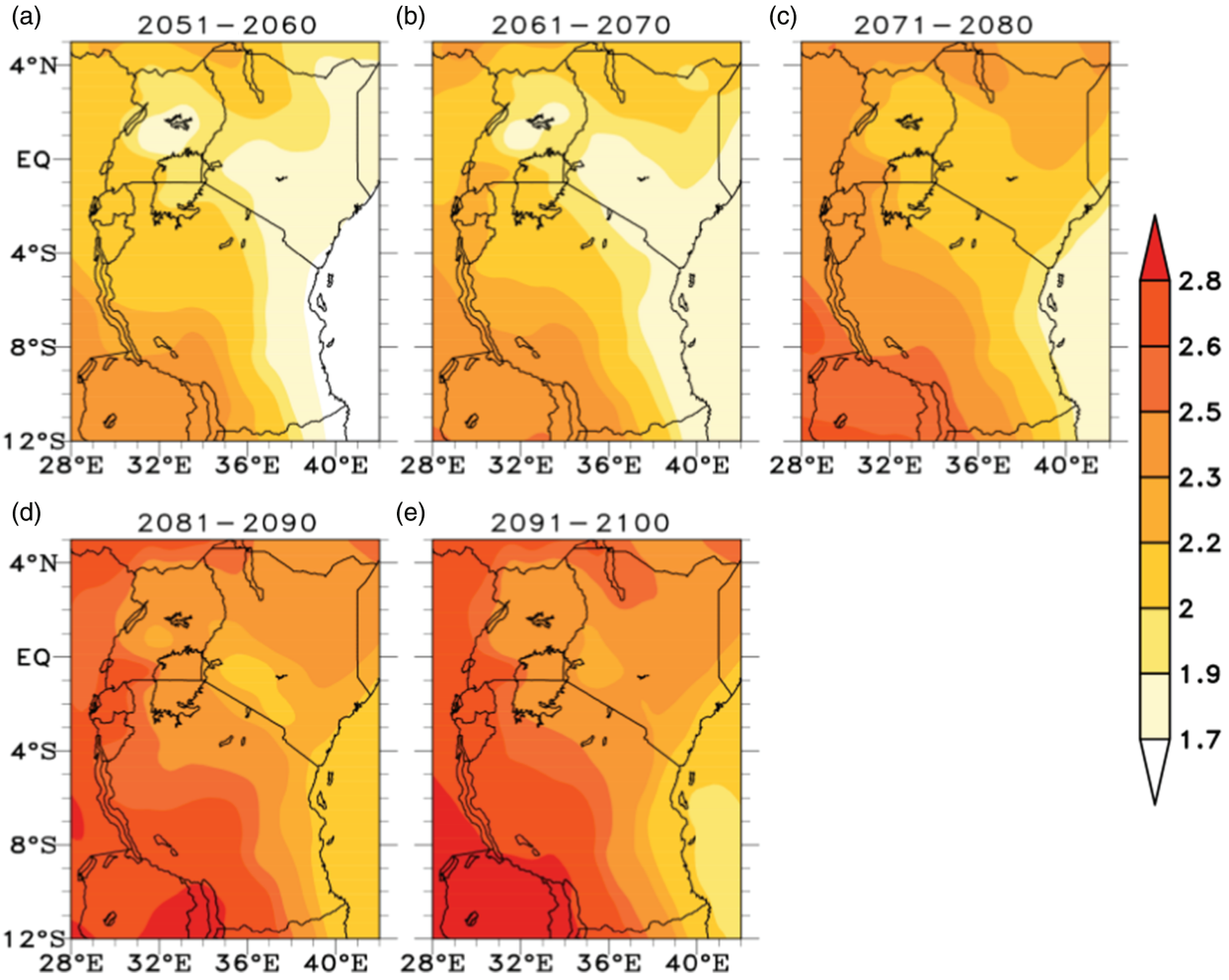

Figure 16. CMIP5 model ensemble mean temperature change (°C) projected under RCP4.5 for 2051–2060 (2050s), 2061–2070 (2060s), 2071–2080 (2070s), 2081–2090 (2080s), and 2091–2100 (2090s) relative to the baseline period (1961–1990).

tourism, which are weather/climate-dependent. The results of this study support the observations made by Adhikari *et al.* (2015) over the entire eastern region of Africa and indicate that the grain crops in the region are likely to be the most affected by ongoing global warming if 'business remains as usual'. That study indicates that wheat is the most vulnerable crop; with a predicted yield reduction of 72% by the end of the 21st century.

Climate change will hinder socioeconomic progress globally, and developing countries will be affected the

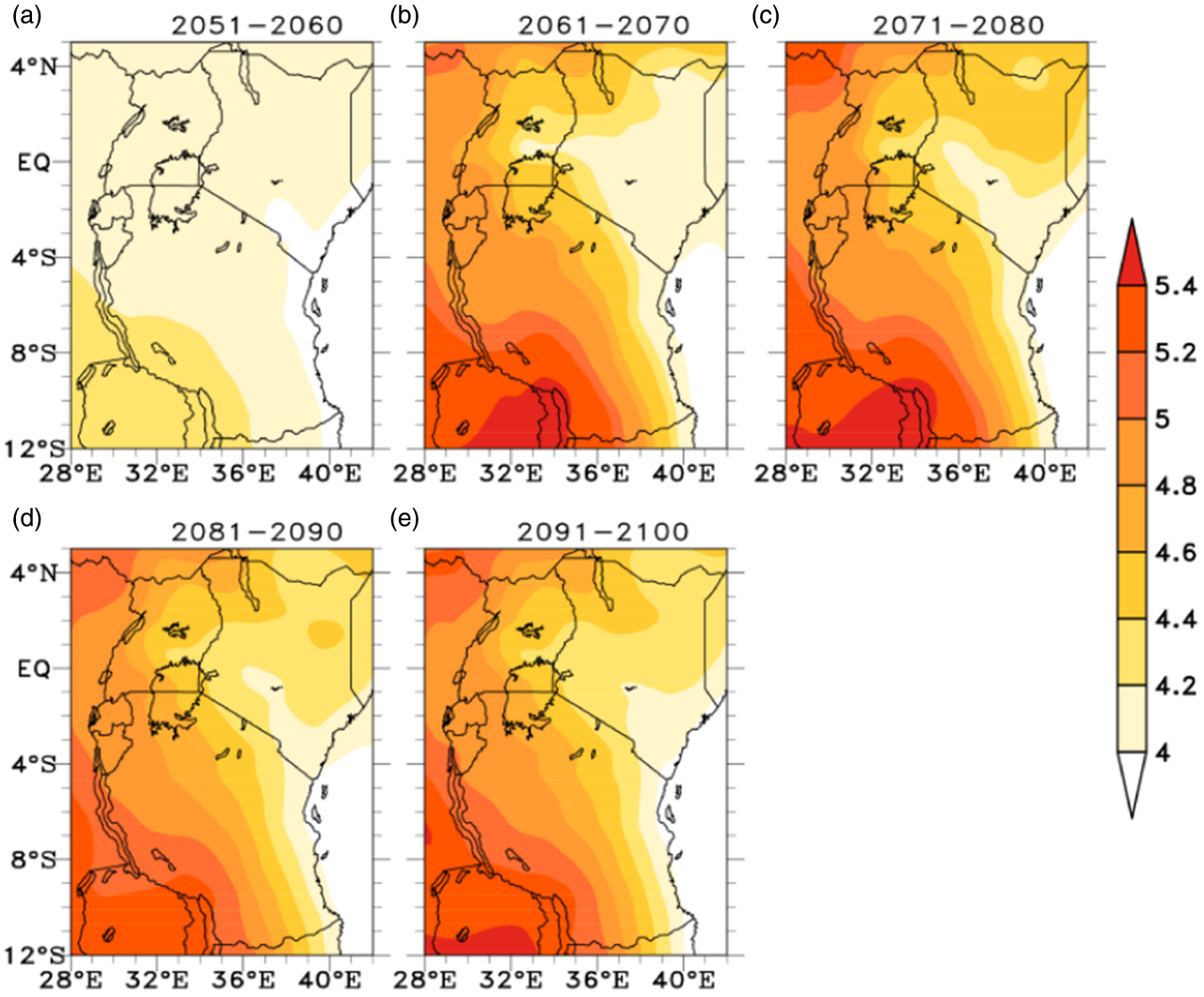

Figure 17. CMIP5 model ensemble mean temperature change (°C) projected under RCP8.5 for 2051–2060 (2050s), 2061–2070 (2060s), 2071–2080 (2070s), 2081–2090 (2080s), and 2091–2100 (2090s) relative to the baseline period (1961–1990). [Colour figure can be viewed at wileyonlinelibrary.com].

Table 5. Sen's slope (mm year^{-1}) of the projected annual rainfall over the EA homogeneous rainfall zones based on CMIP5 ensemble mean data for 2006–2100.

Region	Scenario	
	RCP4.5	RCP8.5
R1	0.86	1.50
R2	1.10	2.30
R3	2.00	3.30
R4	0.90	1.77
R5	0.94	1.53
R6	1.42	2.67
R7	0.72	2.27
R8	1.46	2.99

most (Mendelsohn *et al.*, 2006; Oppenheimer *et al.*, 2014). Thus, it is important to understand the future climate for planning purposes. In this study, rainfall and temperature projections were analysed for EA in the 21st century by using the historical run and the projections under the RCP4.5 and RCP8.5 scenarios. The results suggest that rainfall and temperature will increase in the 21st century relative to the 20th century. For temperature, the change is likely to reach +0.2 and +0.5 °C decade^{-1} between 2006 and 2100 under the RCP4.5 and RCP8.5 scenarios, respectively. The projected warming during the last half of the 21st century relative to the climatological period is likely to range from 1.7 to 2.8 °C and from 2.2 to 5.4 °C under the RCP4.5 and RCP8.5 scenarios, respectively. The highest warming will occur in western Tanzania and northern Kenya. Over the entire study area, the projected temperature showed a remarkable increase in variance as the RCP increased. Scenario uncertainty is projected to be dominant over model uncertainty from the middle to the end of the 21st century.

For rainfall, the increase will be higher under the RCP8.5 scenario than under the RCP4.5 scenario. The mean percentage change in rainfall is projected to be higher during OND, with values of 7.7 and 13.1%, than during MAM, with values of 7.4 and 10.3% for RCP4.5 and RCP8.5.

Table 6. Summary statistics of the MK test for the projected annual temperature (for 2006–2100) over EA under the RCP4.5 and RCP8.5 scenarios.

Scenario	Min (°C)	Max (°C)	Mean (°C)	Std. dev.	*Z*	Sen's slope
RCP4.5	22.98	25.49	24.51	0.63	12.13*	0.02
RCP8.5	23.25	27.65	25.26	1.31	13.45*	0.05

*Significant at the 5% significance level.

Nearly the entire EA will experience a positive change in rainfall. In both scenarios, positive anomalies are concentrated in the central Kenya highlands and extend to the Lake Victoria region. The PDFs of seasonal rainfall show an increase in the frequency of occurrence of what in the baseline period would be extreme wet seasons and years.

The timing, amount, and frequency of rainfall events are important for planning purposes. The monthly distribution of rainfall is highly important in EA, whose economy mainly relies on rain-fed agriculture. The main food crops grown in this area are maize, bean, and millet, which are mainly planted during the 'long rains' season; however, a few farm activities are performed during the 'short rains' season (Amissah-Arthur *et al.*, 2002). Although the projected changes in rainfall seem to favour the agroecological sector, warming and other climatic and non-climatic factors could be important. For instance, despite projecting an increase in rainfall, Thornton *et al.* (2011) indicated that reduction in soil moisture content as a result of warming could decrease agricultural production. Moreover, increasing rainfall can correspond with an increased number of extreme rainfall events that can result in large socioeconomic losses if they are not well planned for.

This study and many other studies have projected that rainfall will increase in EA, in contrast to the observed reductions in MAM and the current increase in the number of drought events (Liebmann *et al.*, 2014; Lyon, 2014; Rowell *et al.*, 2015). This result is called the 'East African climate paradox' (Rowell *et al.*, 2015) and is challenging for the development of climate adaptation plans. Yang *et al.* (2014, 2015b) observed that models exhibit chronic biases in simulating rainfall and tropical responses to raising GHGs. This therefore shows that the rainfall projections made using the same models should be treated with caution, especially as far as long term planning is concerned.

In the context of the ongoing climate change where use of climate information is very helpful, multi-disciplinary co-operation in the climate projection and planning processes is needed to build the confidence of users regarding the accuracy and reliability of climate products. However, in agreement with Rowell *et al.* (2015), this would require process-based skilful assessments of the reliability of EA projections as well as better models of the impacts of aerosol on rainfall. Although obtaining this information may be demanding in terms of resources, it is a worthy investment that should be considered by the affected countries under the umbrella of regional research bodies such as the meteorology arm of the East Africa Community (EAC; http://www.eac.int/sectors/infrastructure/ meteorology) and Intergovernmental Authority on Development (IGAD) Climate Prediction and Applications Centre (ICPAC; www.icpac.net/).

Notably, these results only provide an indication of the expected climate condition and may over/underestimate the actual quantities. Errors are expected due to the models' course resolution and the consideration of a narrow range of GCMs. A narrow range of GCMs tends to underestimate the total uncertainty in various emission scenarios. Thus, it is important that the presented results herein are used cautiously in further studies and for long-term policy planning. Further, there remains need for understanding why most global models perform poorly in reproducing rainfall over EA.

Acknowledgements

This work was supported by the Priority Academic Program Development (PAPD) of Jiangsu Higher Education Institutions through the second author. Sincere appreciation goes to Canadian Climate Data and Scenarios and the respective modelling groups for providing the CMIP5 data. The authors are indebted to Nanjing University of Information Science and Technology (NUIST) for hosting them and for providing all the required facilities and research equipment for completing this work. The first author acknowledges the financial support of the Chinese Scholarship Council (CSC) for his study in China.

References

Adhikari U, Nejadhashemi AP, Woznicki SA. 2015. Climate change and Eastern Africa: a review of impact on major crops. *Food Energy Secur.* **4**: 110–132. https://doi.org/10.1002/fes3.61.

Amissah-Arthur A, Jagtap S, Rosenzweig C. 2002. Spatiotemporal effects of El Niño events on rainfall and maize yield in Kenya. *Int. J. Climatol.* **22**: 1849–1860. https://doi.org/10.1002/joc.858.

Anyah RO, Qiu W. 2012. Characteristic 20th and 21st century precipitation and temperature patterns and changes over the Greater Horn of Africa. *Int. J. Climatol.* **32**: 347–363. https://doi.org/10.1002/joc.2270.

Anyah RO, Semazzi FHM. 2006. Climate variability over the Greater Horn of Africa based on NCAR AGCM ensemble. *Theor. Appl. Climatol.* **86**: 39–62. https://doi.org/10.1007/s00704-005-0203-7.

Behera SK, Luo J-J, Masson S, Delecluse P, Gualdi S, Navarra A, Yamagata T. 2005. Paramount impact of the Indian Ocean dipole on the East African short rains: ACGCM study. *J. Clim.* **18**: 4514–4530. https://doi.org/10.1175/JCLI3541.1.

Bernacchia A, Pigolotti S. 2011. Self-consistent method for density estimation. *J. R. Stat. Soc. Ser. B: Stat. Methodol.* **73**: 407–422. https://doi.org/10.1111/j.1467-9868.2011.00772.x.

Black E, Slingo J, Sperber K. 2003. An observational study of the relationship between excessively strong short rains in coastal East Africa and Indian Ocean SST. *Mon. Weather Rev.* **131**: 74–94. https://doi.org/10.1175/1520-0493(2003)131<0074:AOSOTR>2.0.CO;2.

Camberlin P. 2017. Temperature trends and variability in the Greater Horn of Africa: interactions with precipitation. *Clim. Dyn.* **48**: 477–498. https://doi.org/10.1007/s00382-016-3088-5.

Camberlin P, Okoola RE. 2003. The onset and cessation of the 'long rains' in eastern Africa and their interannual variability. *Theor. Appl. Climatol.* **54**: 43–54. https://doi.org/10.1007/s00704-002-0721-5.

Camberlin P, Philippon N. 2002. The East African March–May rainy season: associated atmospheric dynamics and predictability over the 1968–97 period. *J. Clim.* **15**: 1002–1019. https://doi.org/10.1175/1520-0442(2002)015<1002:TEAMMR>2.0.CO;2.

Camberlin P, Wairoto JG. 1997. Intraseasonal wind anomalies related to wet and dry spells during the "long" and "short" rainy seasons in Kenya. *Theor. Appl. Climatol.* **58**: 57–69. https://doi.org/10.1007/BF00867432.

Christensen JH, Krishna Kumar K, Aldrian E, An S-I, IFA C, de Castro M, Dong W, Goswami P, Hall A, Kanyanga JK, Kitoh A, Kossin J, Lau N-C, Renwick J, Stephenson DB, Xie S-P, Zhou T. 2013. Climate phenomena and their relevance for future regional climate change. In *Climate Change 2013: The Physical Science Basis. Contribution of Working Group I to the Fifth Assessment Report of the Intergovernmental Panel on Climate Change*, Stocker TF, Qin D, Plattner G-K, Tignor M, Allen SK, Boschung J, Nauels A, Xia Y, Bex V, Midgley PM (eds). Cambridge University Press: Cambridge, UK and New York, NY.

Dike VN, Shimizu MH, Diallo M, Lin Z, Nwofor OK, Chineke TC. 2015. Modelling present and future African climate using CMIP5 scenarios in HadGEM2-ES. *Int. J. Climatol.* **35**: 1784–1799. https://doi.org/10.1002/joc.4084.

Engelbrecht F, Adegoke J, Bopape M-J, Naidoo M, Garland R, Thatcher M, McGregor J, Katzfey J, Werner M, Ichoku C, Gatebe C. 2015. Projections of rapidly rising surface temperatures over Africa under low mitigation. *Environ. Res. Lett.* **10**(8): 085004. https://doi.org/10.1088/1748-9326/10/8/085004.

Gamoyo M, Reason C, Obura D. 2015. Rainfall variability over the East African coast. *Theor. Appl. Climatol.* **120**: 311–322. https://doi.org/10.1007/s00704-014-1171-6.

Hastenrath S, Nicklis A, Greischar L. 1993. Atmospheric-hydrospheric mechanisms of climate anomalies in the western equatorial Indian Ocean. *J. Geophys. Res.* **98**: 20219–20235. https://doi.org/10.1029/93JC02330.

Hastenrath S, Polzin D, Mutai C. 2007. Diagnosing the 2005 drought in equatorial East Africa. *J. Clim.* **20**: 4628–4637. https://doi.org/10.1175/JCLI4238.1.

Hawkins E, Sutton R. 2009. The potential to narrow uncertainty in regional climate predictions. *Bull. Am. Meteorol. Soc.* **90**: 1095–1107. https://doi.org/10.1175/2009BAMS2607.1.

Hawkins E, Sutton R. 2011. The potential to narrow uncertainty in projections of regional precipitation change. *Clim. Dyn.* **37**: 407–418. https://doi.org/10.1007/s00382-010-0810-6.

Hibbard KA, Van Vurren DP, Edmonds J. 2011. A primer on the representative concentration pathways (RCPs) and the coordination between the climate and integrated assessment modelling communities. *CLIVAR Exch.* **16**: 12–15.

Indeje M, Semazzi FHM, Ogallo LJ. 2000. ENSO signals in East African rainfall seasons. *Int J. Climatol.* **20**: 19–46. https://doi.org/10.1002/(SICI)1097-0088(200001)20:1<19::AID-JOC449>3.0.CO;2-0.

Indeje M, Semazzi FHM, Xie L, Ogallo LJ. 2001. Mechanistic model simulations of the East African climate using NCAR regional climate model: influence of large-scale orography on the Turkana low-level jet. *J. Clim.* **14**: 2710–2724. https://doi.org/10.1175/1520-0442(2001)014<2710:MMSOTE>2.0.CO;2.

IPCC. 2001. In *Climate Change 2001: Impacts, Adaptation and Vulnerability, Contribution of Working Group II to the Third Assessment Report of the Intergovernmental Panel on Climate Change*, McCarthy JJ, Canziani OF, Leary NA, Dokken DJ, White KS (eds). Cambridge University Press: Cambridge, UK and New York, NY, 1032.

IPCC. 2007. In *Climate Change 2007: The Physical Science Basis. Contribution of Working Group I to the Fourth Assessment Report of the Intergovernmental Panel on Climate Change*, Solomon S, Qin D, Manning M, Chen Z, Marquis M, Averyt KB, Tignor M, Miller HL (eds). Cambridge University Press: Cambridge, UK and New York, NY, 996.

Jakob C. 2010. Accelerating progress in global atmospheric model development through improved parameterizations: challenges, opportunities, and strategies. *Bull. Am. Meteorol. Soc.* **91**: 869–875. https://doi.org/10.1175/2009BAMS2898.1.

Kendall MG. 1975. *Rank Correlation Methods*, 4th edn. Griffin: London.

Kent C, Chadwick R, Rowell DP. 2015. Understanding uncertainties in future projections of seasonal tropical precipitation. *J. Clim.* **28**: 4390–4413. https://doi.org/10.1175/JCLI-D-14-00613.1.

Kijazi AL, Reason CJC. 2009a. Analysis of the 2006 floods over northern Tanzania. *Int. J. Climatol.* **29**: 955–970. https://doi.org/10.1002/joc.1846.

Kijazi AL, Reason CJC. 2009b. Analysis of the 1998 to 2005 drought over the northeastern highlands of Tanzania. *Clim. Res.* **38**: 209–223. https://doi.org/10.3354/cr00784.

Kizza M, Rodhe A, Xu C-Y, Ntale HK, Halldin S. 2009. Temporal rainfall variability in the Lake Victoria Basin in East Africa during the twentieth century. *Theor. Appl. Climatol.* **98**: 119–135. https://doi.org/10.1007/s00704-008-0093-6.

Klein F, Goosse H, Graham NE, Verschuren D. 2016. Comparison of simulated and reconstructed variations in East African hydroclimate over the last millennium. *Clim. Past* **12**: 1499–1518. https://doi.org/10.5194/cp-12-1499-2016.

Knutti R, Sedláček J. 2013. Robustness and uncertainties in the new CMIP5 climate model projections. *Nat. Clim. Change* **3**: 369–373. https://doi.org/10.1038/nclimate1716.

Liebmann B, Hoerling MP, Funk C, Bladé I, Dole RM, Allured D, Quan X, Pegion P, Eischeid JK. 2014. Understanding recent eastern Horn of Africa rainfall variability and change. *J. Clim.* **27**: 8630–8645. https://doi.org/10.1175/JCLI-D-13-00714.1.

Lyon B. 2014. Seasonal drought in Greater Horn of Africa and its recent increase during the March–May long rains. *J. Clim.* **27**: 7953–7975. https://doi.org/10.1175/JCLI-D-13-00459.1.

Lyon B, Dewitt DG. 2012. A recent and abrupt decline in the East African long rains. *Geophys. Res. Lett.* **39**(2): L02702. https://doi.org/10.1029/2011GL050337.

Maidment RI, Allan RP, Black E. 2015. Recent observed and simulated changes in precipitation over Africa. *Geophys. Res. Lett.* **42**: 8155–8164. https://doi.org/10.1002/2015GL065765.

Manatsa D, Chipindu B, Behera SK. 2012. Shifts in IOD and their impacts on association with East Africa rainfall. *Theor. Appl. Climatol.* **110**: 115–128. https://doi.org/10.1007/s00704-012-0610-5.

Mann BH. 1945. Nonparametric tests against trend. *Econometrica* **13**: 245–259.

Mendelsohn R, Dinar A, Williams L. 2006. The distributional impact of climate change on rich and poor countries. *Environ. Dev. Econ.* **11**: 159–178. https://doi.org/10.1017/S1355770X05002755.

Moss RH, Edmonds JA, Hibbard KA, Manning MR, Rose SK, Van Vuuren DP, Carter TR, Emori S, Kainuma M, Kram T, Meehl GA, Mitchell JFB, Nakicenovic N, Riahi K, Smith SJ, Stouffer RJ, Thomson AM, Weyant JP, Wilbanks TJ. 2010. The next generation of scenarios for climate change research and assessment. *Nature* **463**: 747–756. https://doi.org/10.1038/nature08823.

Mutai CC, Ward MN. 2000. East African rainfall and the tropical circulation/convection on intraseasonal to interannual timescales. *J. Clim.* **13**: 3915–3939. https://doi.org/10.1175/1520-0442(2000)013<3915:EARATT>2.0.CO;2.

Mutai CC, Ward MN, Colman AW. 1998. Towards the prediction of East African short rains based on sea surface temperature-atmosphere coupling. *Int. J. Climatol.* **18**: 975–997. https://doi.org/10.1002/(SICI)1097-0088(199807)18:9<975::AID-JOC259>3.0.CO;2-U.

Muthama NJ, Masieyi WB, Okoola RE, Opere AO, Mukabana JR, Nyakwada W, Aura S, Chanzu BA, Manene MM. 2012. Survey on the utilization of weather information and products for selected districts in Kenya. *J. Meteorol. Relat. Sci.* **6**: 51–58.

Niang I, Ruppel OC, Abdrabo MA, Essel A, Lennard C, Padgham J, Urquhart P. 2014. Africa. In *Climate Change 2014: Impacts, Adaptation, and Vulnerability. Part B: Regional Aspects. Contribution of Working Group II to the Fifth Assessment Report of the Intergovernmental Panel on Climate Change*, Barros VR, Field CB, Dokken DJ, Mastrandrea MD, Mach KJ, Bilir TE, Chatterjee M, Ebi KL, Estrada YO, Genova RC, Girma B, Kissel ES, Levy AN, MacCracken S, Mastrandrea PR, White LL (eds). Cambridge University Press: Cambridge, UK and New York, NY, 1199–1265.

Nicholson SE. 2014. A detailed look at the recent drought situation in the Greater Horn of Africa. *J. Arid Environ.* **103**: 71–79. https://doi.org/10.1016/j.jaridenv.2013.12.003.

Nicholson SE. 2016. An analysis of recent rainfall conditions in eastern Africa. *Int. J. Climatol.* **36**: 526–532. https://doi.org/10.1002/joc.4358.

Nsubuga FNW, Olwoch JM, de Rautenbach CJW, Botai OJ. 2014a. Analysis of mid-twentieth century rainfall trends and variability over southwestern Uganda. *Theor. Appl. Climatol.* **115**: 53–71. https://doi.org/10.1007/s00704-013-0864-6.

Nsubuga FW, Olwoch JM, Rautenbach H. 2014b. Variability properties of daily and monthly observed near-surface temperatures in Uganda: 1960–2008. *Int. J. Climatol.* **34**: 303–314. https://doi.org/10.1002/joc.3686.

Oettli P, Camberlin P. 2005. Influence of topography on monthly rainfall distribution over East Africa. *Clim. Res.* **28**: 199–212. https://doi.org/10.3354/cr028199.

Ogallo LJ. 1988. Relationships between seasonal rainfall in East Africa and the southern oscillation. *J. Climatol.* **8**: 31–43. https://doi.org/10.1002/joc.3370080104.

Ogwang BA. 2015. *Simulation and Prediction of the East African Climate Using Regional Climate Model (RegCM4)*. PhD thesis, Nanjing University of Information Science and Technology, Nanjing, China.

Ogwang BA, Chen H, Li X, Gao C. 2014. The influence of topography on East African October to December climate: sensitivity experiments with RegCM4. *Adv. Meteorol.* **2014**: 143917. https://doi.org/10.1155/2014/143917.

Okoola R. 1999. A diagnostic study of the eastern African monsoon circulation during the northern hemisphere spring season. *Int. J. Climatol.* **19**: 143–168. https://doi.org/10.1002/(SICI)1097-0088(199902)19:2<143::AID-JOC342>3.0.CO;2-U.

Omondi PA, Awange JL, Forootan E, Ogallo LA, Barakiza R, Girmaw GB, Fesseha I, Kululetera V, Kilembe C, Mbati MM, Kilavi M, King'uyu SM, Omeny PA, Njogu A, Badr EM, Musa TA, Muchiri P, Bamanya D, Komutunga E. 2014. Changes in temperature and precipitation extremes over the Greater Horn of Africa region from 1961 to 2010. *Int. J. Climatol.* **34**: 1262–1277. https://doi.org/10.1002/joc.3763.

Omumbo JA, Lyon B, Waweru SM, Connor SJ, Thomson MC. 2011. Raised temperatures over the Kericho tea estates: revisiting the climate in the East African highlands malaria debate. *Malar. J.* **10**: 12. https://doi.org/10.1186/1475-2875-10-12.

Ongoma V, Chen H. 2017. Temporal and spatial variability of temperature and precipitation over East Africa from 1951 to 2010. *Meteorol. Atmos. Phys.* **129**: 131–144. https://doi.org/10.1007/s00703-016-0462-0.

Ongoma V, Muthama JN, Gitau W. 2013. Evaluation of urbanization on urban temperature of Nairobi City, Kenya. *Global Meteorol.* **2**(e1). https://doi.org/10.4081/gm.2013.e1.

Ongoma V, Chen H, Gao C. 2016a. Evaluation of CMIP5 GCMs 20th century climate simulations for the equatorial East Africa rainfall based on gridded data. *Theor. Appl. Climatol.* (in press).

Ongoma V, Chen H, Omony GW. 2016b. Variability of extreme weather events over East Africa, a case study of rainfall in Kenya and Uganda. *Theor. Appl. Climatol.* https://doi.org/10.1007/s00704-016-1973-9.

Oppenheimer M, Campos M, Warren R, Birkmann J, Luber G, O'Neill B, Takahashi K. 2014. Emergent risks and key vulnerabilities. In *Climate Change 2014: Impacts, Adaptation, and Vulnerability. Part A: Global and Sectoral Aspects. Contribution of Working Group II to the Fifth Assessment Report of the Intergovernmental Panel on Climate Change*, Field CB, Barros VR, Dokken DJ, Mach KJ, Mastrandrea MD, Bilir TE, Chatterjee M, Ebi KL, Estrada YO, Genova RC, Girma B, Kissel ES, Levy AN, MacCracken S, Mastrandrea PR, White LL (eds). Cambridge University Press: Cambridge, UK and New York, NY, 1039–1099.

Otieno VO, Anyah RO. 2013. CMIP5 simulated climate conditions of the Greater Horn of Africa (GHA). Part II. Projected climate. *Clim. Dyn.* **41**: 2099–2113. https://doi.org/10.1007/s00382-013-1694-z.

Owiti Z, Zhu W. 2012. Spatial distribution of rainfall seasonality over East Africa. *J. Geogr. Reg. Plann.* **5**: 409–421. https://doi.org/10.5897/JGRP12.027.

Patricola CM, Cook KH. 2011. Sub-Saharan northern African climate at the end of the twenty-first century: forcing factors and climate change processes. *Clim. Dyn.* **37**: 1165–1188. https://doi.org/10.1007/s00382-010-0907-y.

Riahi K, Rao S, Krey V, Cho C, Chirkov V, Fischer G, Kindermann G, Nakicenovic N, Rafaj P. 2011. RCP8.5 – a scenario of comparatively high greenhouse gas emissions. *Clim. Change* **109**: 33–57. https://doi.org/10.1007/s10584-011-0149-y.

Rowell DP, Booth BBB, Nicholson SE, Good P. 2015. Reconciling past and future rainfall trends over East Africa. *J. Clim.* **28**: 9768–9788. https://doi.org/10.1175/JCLI-D-15-0140.1.

Schmocker J, Liniger HP, Ngeru JN, Brugnara Y, Auchmann R, Brönnimann S. 2016. Trends in mean and extreme precipitation in the Mount Kenya region from observations and reanalyses. *Int. J. Climatol.* **36**: 1500–1514,doi. https://doi.org/10.1002/joc.4438.

Segele ZT, Lamb PJ, Leslie LM. 2009. Large-scale atmospheric circulation and global sea surface temperature associations with Horn of Africa June–September rainfall. *Int. J. Climatol.* **29**: 1075–1100. https://doi.org/10.1002/joc.1751.

Sen PK. 1968. Estimates of the regression coefficient based on Kendall's tau. *J. Am. Stat. Assoc.* **63**: 1379–1389. https://doi.org/10.1080/01621459.1968.10480934.

Seneviratne SI, Nicholls N, Easterling D, Goodess CM, Kanae S, Kossin J, Luo Y, Marengo J, McInnes K, Rahimi M, Reichstein M, Sorteberg A, Vera C, Zhang X. 2012. Changes in climate extremes and their impacts on the natural physical environment. In *Managing the Risks of Extreme Events and Disasters to Advance Climate Change Adaptation. A Special Report of Working Groups I and II of the Intergovernmental Panel on Climate Change*, Field CB, Barros V, Stocker TF, Qin D, Dokken DJ, Ebi KL, Mastrandrea MD, Mach KJ, Plattner G-K, Allen SK, Tignor M, Midgley PM (eds). Cambridge University Press: Cambridge, UK and New York, NY, 109–230.

Shongwe ME, van Oldenborgh GJ, van den Hurk B, van Aalst M. 2011. Projected changes in mean and extreme precipitation in Africa under global warming. Part II: East Africa. *J. Clim.* **24**: 3718–3733. https://doi.org/10.1175/2010JCLI2883.1.

Snedecor GW, Cochran WG. 1989. *Statistical Methods*, 8th edn. Iowa State University Press: Iowa City, IA.

Stern DI, Gething PW, Kabaria CW, Temperley WH, Noor AM, Okiro EA, Shanks GD, Snow RW, Hay SI. 2011. Temperature and malaria trends in highland East Africa. *PLoS One* **6**: e24524. https://doi.org/10.1371/journal.pone.0024524.

Taylor KE, Stouffer RJ, Meehl GA. 2012. An overview of CMIP5 and the experiment design. *Bull. Am. Meteorol. Soc.* **93**: 485–498. https://doi.org/10.1175/BAMS-D-11-00094.1.

Theil H. 1950. A rank-invariant method of linear and polynomial regression analysis. I, II, III. *Proc. R. Netherlands Acad. Sci.* **53**: 386, 521, 1397–392, 525, 1412.

Thomson AM, Calvin KV, Smith SJ, Kyle GP, Volke A, Patel P, Delgado-Arias S, Bond-Lamberty B, Wise MA, Clarke LE, Edmonds JA. 2011. RCP4.5: a pathway for stabilization of radiative forcing by 2100. *Clim. Change* **109**: 77–94. https://doi.org/10.1007/s10584-011-0151-4.

Thornton PK, Jones PG, Ericksen PJ, Challinor AJ. 2011. Agriculture and food systems in sub-Saharan Africa in a 4 °C+ world. *Philos. Trans. R. Soc. A* **369**: 117–136. https://doi.org/10.1098/rsta.2010.0246.

Tierney JE, Ummenhofer CC, deMenocal PB. 2015. Past and future rainfall in the Horn of Africa. *Sci. Adv.* **1**: e1500682. https://doi.org/10.1126/sciadv.1500682.

University of East Anglia Climatic Research Unit, Harris IC, Jones PD. 2014. *CRU TS3.22: Climatic Research Unit (CRU) Time-Series (TS) Version 3.22 of High Resolution Gridded Data of Month-by-month Variation in Climate (Jan. 1901–Dec. 2013)*. NCAS British Atmospheric Data Centre: Harwell Oxford. https://doi.org/10.5285/18BE23F8-D252-482D-8AF9-5D6A2D40990C.

Williams A, Funk C. 2011. A westward extension of the warm pool leads to a westward extension of the Walker circulation, drying eastern Africa. *Clim. Dyn.* **37**: 2417–2435. https://doi.org/10.1007/s00382-010-0984-y.

Williams AP, Funk C, Michaelsen J, Rauscher SA, Robertson I, Wils THG, Koprowski M, Eshetu Z, Loader NJ. 2012. Recent summer precipitation trends in the Greater Horn of Africa and the emerging role of Indian Ocean sea surface temperature. *Clim. Dyn.* **39**: 2307–2328. https://doi.org/10.1007/s00382-011-1222-y.

World Bank. 2008. *The Growth Report: Strategies for Sustained Growth and Inclusive Development*. Commission on Growth and Development, World Bank: Washington, DC.

Yang W, Seager R, Cane MA, Lyon B. 2014. The East African long rains in observations and models. *J. Clim.* **27**: 7185–7202. https://doi.org/10.1175/JCLI-D-13-00447.1.

Yang W, Seager R, Cane MA, Lyon B. 2015a. The annual cycle of East African precipitation. *J. Clim.* **28**: 2385–2404. https://doi.org/10.1175/JCLI-D-14-00484.1.

Yang W, Seager R, Cane MA, Lyon B. 2015b. The rainfall annual cycle bias over East Africa in CMIP5 coupled climate models. *J. Clim.* **28**: 9789–9802. https://doi.org/10.1175/JCLI-D-15-0323.1.

